TO INVESTIGATE THE ROLE OF ADDITIVES ON THE FLOW CHARACTERISTICS OF FLY ASH SLURRY AT HIGH CONCENTRATION

Submitted in partial fulfillment of the requirements for the award of degree of

Master of Engineering

In

Thermal Engineering

Submitted by

RAJIV GILL

Roll No: 801183018

Under the guidance of

Mr. Kundan Lal

Assistant Professor

Mechanical Engineering Department

Thapar University, Patiala

MECHANICAL ENGINEERING DEPARTMENT

THAPAR UNIVERSITY, PATIALA-147004

JUNE, 2013

i

AUTHOR'S DECLARATION

I, "**Rajiv Gill**", hereby declare that the work which is being presented in this thesis entitled "**To investigate the role of additives on the flow characteristics of fly ash slurry at high concentrations**" by me in partial fulfillment of the requirements for the award of degree of Master of Engineering in Thermal engineering from Thapar University, Patiala, is an authentic record carried out under the supervision of **Mr. Kundan Lal, Assistant Professor, MED, Thapar University, Patiala.**

The matter embodied in this thesis has not been submitted in any other University/Institute for the award of any other degree.

Date: 15/07/13

RGill
(RAJIV GILL)

Reg. No. 801183018

This is certify that the above statement made by the student concerned is correct to the best of my knowledge and belief.

Date:

(Mr. KUNDAN LAL)

Assistant Professor

Mechanical Engineering Department

Thapar University, Patiala

Countersigned by:

(Dr. AJAY BATISH)

Professor and Head

Mechanical Engineering Deparment

Patiala-147004

(Dr. S.K.MOHAPATRA)

DOAA & Senior Professor

Thapar University

Patiala- 147004

ABSTRACT

Coal based thermal power plants all over the world face serious problems of handling and disposal of the fly ash produced. Thermal power stations use pulverized coal as fuel. They produce enormous quantitative of coal ash as a by- product of combustion. The high ash content (30-50%) of the coal in India makes this problem more complex. Transportation of fly ash is a major problem in its efficient disposal. The main problem associated with fly ash transportation is that the particles settle down sooner than desired. The primary objective of this research is that not only the fly ash particles should remain floated till it reaches the end but also settle down after that. In this investigation the role of a drag-reducing (additives) has been evaluated to achieve the objectives. The additive used are detergent Ariel which act as an anionic surfactant in nature, Glycerol and polyethylene glycol (reffered as PEG) which are act as a non-anionic surfactacts in nature and anionic sodium lauryl sulfate (reffered as SLS).The action of different these additives on flow behaviour of slurry is studied at different dosage using a rheometer.. Effect of 3 concentrations of additives (0.5%, 1% and 1.5% by weight) on viscosity of 40%, 50%, 60% and 65% fly ash slurry is studied. The effective design, control and safe operation of a slurry hydraulic transport system require the successful prediction of slurry flow behavior in the pipeline. To study the good flow behaviour is to matching the actual data with rheological models (Bingham's model, Power law's model and Harschel-Bulkley model) values. Slurry flow behavior is not only dependent on the properties of both solids and carrier, but also it is strongly affected by mutual particle-particle and particle liquid interaction. Rheological models are excellent mathematical tools which help to analyze good flow behaviour. Study indicates that, additives of different nature (anionic and non-ionic surfactant) help reduce viscosity and shear stress of slurry which leads to decrease in specific power consumption and increase overall the transport system efficiency. Particle size distribution plays an important role to obtain higher concentrated slurries and higher carrying capacity. In this work, the particles of different size range are extracted through mechanical sieving and flow behaviour of slurries at 53-106µm is made at different concentrations. The study relivance the large particle size adversely affects flow behavior**.**

ACKNOWLEDGEMENT

I express my sincere gratitude to my supervisor **Mr. Kundan Lal, Assistant Professor, Mechanical Engineering Department, Thapar University, Patiala**, for his continuous support and guidance during last two years, without him this work could not be completed. I am thankful for his patience and cooperation. I also appreciates his effort in thoroughly revising the thesis, and thankful to him sharing valuable experience and suggestions.

I am sincerely thankful to **Mr. Satish Kumar** (Assistant Professor, MED) for helping me in my work with his lab facilities. I would also like to thank Mr. Prince Kumar Gogia (JRF mechanical dept.) for helping me with my experiments on rheometer and Mr. Arunanshu Chakarvarty for sharing his valuable knowledge with me. I am thankful to **Dr. Monika Saini, SMCA Dept**. for guiding me through my work. I express my gratitude to Dr. Ajay Batish (HOD Mechanical dept.) for his fast and sincere to my applications each and every time. Furthermore, I am grateful to my friends who came across and supported at every step. Lastly, I am thankful to my parents for their patience and understanding and also for the continuous encouragement they gave me in my rough times.

Last but not the least; I would like to thank the God for all his good benevolence.

(RAJIV GILL)

INDEX

CONTENTS Page No.

List of Figures

List of Tables

CHAPTER 1

INTRODUCTION

1.1 Need to utilize of fly ash

Coal based thermal power stations have been operational for than 55 years but the concept of developing environment friendly solutions for fly ash utilization is only about 15 years old. The increase in fly ash utilization from one million tonne during (1993-1994) to 70 million tonne levels (2007-2008) are though quite satisfying but the quantum of un-utilized fly ash also increased from 39 million tonne per year to 60 million tonne per year for this period [15]. It is projected that coal would continue to remain the major source of energy for power generation in the country. The estimates prepared by ministry of power as well as planning commissions up to the year 2031-2032 indicate that the coal requirement and generation of fly ash during the year 2031-2032 would be around 1800 million tonne and 600 million tonne respectively [15,20]. The problems of effective utilization of coal ash have been given attention for at least fifteen years in India. Although the effort devoted to the problems has led to some applications of demonstrated usefulness, the full utilization of coal ash has been hindered by lack of effective knowledge dissemination from field studies to potential users of coal ash, and by the obvious variability of the product. The deposit of a large amount of fly ash and bottom ash discharged from coal-fired power stations is a very serious problem. The amount of fly ash is larger than bottom ash. Considerable amount of recycle use is available, mainly by adding fly ash to cement. However, the addition of fly ash to cement is limited because the production rate of cement is leveled off, and also the concentration of fly ash in cement is limited. Thus, it is expected that large amount of fly ash must be transported from power stations to waste material deposit site in the near future. The deposit sites are not necessarily located near the power stations. Long distance transportation of fly ash with reduced cost must be considered. The design of a pipeline transportation system must be accomplished by means of the design procedure based on precise knowledge of rheological behavior of dense fly ash slurries. Most of the pipelines operating today in thermal power plants transport ash at low or high solid concentrations over short as well as large distances. These systems are very energy intensive and also lead to excessive wear of pipeline and wastage of water. Further, the present enhanced consciousness towards the imbalance in the eco-system and related stringent government policies are forcing the thermal power plants to adopt environment friendly transportation systems. Thus, high concentration slurry disposal (HCSD) system has emerged as preferred option to transport fly ash in thermal power plants as it is economical and environment friendly [26]. Researchers found that at high concentrations above 40% by weight, ash slurries behave like non-settling homogenous slurry and the pipe flow can be maintained in laminar flow at comparatively lower velocities. Thus at low velocities, the pipeline will be subjected to minimum erosion wear. Many advantages of high concentrations slurry transportation such as use of low water and specific energy consumption, absence of contamination of water sources etc. They concluded that the concentration of 50% by weight was the limit of safe pumping of coal ash using a centrifugal pump and positive displacement pumps may become necessary to pump fly ash slurries above this concentration. The knowledge of slurry is very vital particularly in the high concentration slurry transportation. Therefore it is essential to establish the exact rheological nature of fly ash slurries at high concentration. Hydraulic pipelines are mostly used to transport solid particulate materials using water or any other liquid as the carrier fluid. These pipelines are used either for long distance or medium distance transportation of bulk materials.Hydraulic pipelines today have also been accepted by various industries as an attractive mode of solid waste transportation within the plant and outside because of its low maintenance cost and being environment-friendly. In power stations, these pipelines are used prevalently for disposal of fly ash/bottom ash to ash pond area. In India alone, approximately 135 million tones of fly ash are transported every year to disposal sites by pipelines at various power stations situated across the country. However, these pipe lines carry lean slurry concentration with fly ash to water ratio at about 1:20. Therefore such huge quantity of water is transported to the disposal site requiring vast stretch of valuable land area. In India about 65,000 acres of land is lying under the ash ponds [6]. The transported water drains away from the pond area which in turn contaminates the surface water and ground water flow downstream. The presence of solid particles leads to drastic changes in the flow behavior, which in turn affects the pressure drop across the pipeline. Coarse solid particulate slurries require high operating velocities for transportation resulting in higher specific energy consumption per unit solid throughout. On the other hand transportation of non-settling slurries would result in lower energy consumption and better operational conditions. A surfactant is chosen to investigation and added to the fly ash slurry to keep the solid particles water borne in the suspension during its transportation through the hydraulic pipelines. These additives when added to a liquid, reduces its surface tension, thereby increasing its spreading and wetting properties. These aqueous solutions can reduce up to 80% of the drag in a turbulent straight pipe flow in a wide range of temperature environment. Many researchers have investigated the characteristics of such a dilute surfactant solution**,** but limited studies are reported about the use of these additives for the transportation of fly ash slurry in the pipe lines.

1.2 Back ground and history of the study

In the early days of the power generation industry, fly ash is considered to be a waste material. The properties of this material was not studied or evaluated seriously and nearly all of the coal combustion products were landfilled. The product was tested to understand the physical properties, chemical properties and suitability as a construction material. During the past several decades, generation of electricity through various coal combustion processes has grown to increased population and associated industrial and commercial development in the United States and other parts of the world [28]. These coal combustion processes leave behind residue that is referred as fly ash. In the 1920's, most effective methods of firing power plant boilers were invented. These new processes consist burning of pulverized coal instead of lump coal. While the process was a most efficient method of firing, the process generated an increased stream of fine combustion products. Thus, this fine combustion product is called fly ash, and the cinders that are relatively finer are called bottom ash. As environmental awareness and landfilling costs have grown, coal combustion product generators and government regulators have encouraged the beneficial use of industrial by-products, including coal ash. In some parts of the world, combustion product utilization rates are much higher than that of the United States. Coal fired power generation has gone through several process modifications to improve efficiency, to improve the quality of combustion products and control the quality of air emissions. The type of coal that is burned influences the chemistry of combustion products significantly. The presence of low sulfur coal has improved the quality of air emissions and also improved the quality of fly ash. It is important to distinguish fly ash, bottom ash, and other CCPs from incinerator ash. The composition of fly ash and incinerator ash consequently is very different. The composition of fly ash from a single source is very uniform and consistent, unlike the composition of incinerator ash, which varies because of the wide variety of waste materials burned. The disposal cost of CCPs has escalated significantly during the last couple of decades due to significant changes in landfill design regulations. Fly ash and bottom ash are used beneficially as engineered backfill material; this material is replacing sand or gravel that would have been transported from various locations. Coal is one of the most commonly used energy source for the generation of electricity. Coal combustion products are the solid residues that remain after the combustion of coal within a furnace. In the early days of power generation by a coal-fired generating plant, coal was fired in a furnace with stoker grates. Now most coal-fueled power plants are fired with pulverized coal. In the coal combustion process, coal combustion products are also generated in direct proportion to the variety and quantity of coal consumed. The pulverized coal is burned in the furnace to generate and the hot gases then pass through the bank of tubes in the boiler and are eventually cleaned and discharged through the plant chimney. In large power plants consumption of large quantities of coal, large quantities of coal ash are produced. This ash that is collected in electrostatic precipitators or baghouses is called fly ash. In ECPs the flue gas is passed between electrically charged plates where the fly ash particles are then attracted to the plates. Baghouses are used to collect ash with bags that filter the fly ash out of the flue gas stream. The fly ash particles are then knocked off the plates or bags and fall into the hoppers located at the bottom of the electrostatic precipitators or baghouses. After that fly ash is then pneumatically transported to storage silos. The storage silos are equipped with wet unloaders for conditioned ash or disposal applications and dry unloaders for loading dry bulk semi tankers or rail cars. The ash collected from the pulverized coal fired furnaces is fly ash and bottom ash. Fly ash constitutes a major component (80 to 90%) and the bottom ash component is in the range of 10 to 20%. The ash is kept in the molten state and tapped off as a liquid.

1.3 Characterization of fly ash

The properties of fly ash vary with the type of coal used, , the grinding equipment, furnace and the combustion process. ASTM (American Society for Testing and Materials) C618-03 Standard Specification for Coal Fly Ash and Raw classifies fly ash into two categories – Class F and Class C fly ash. Combustion of anthracite or bituminous coal normally produces Class F (low calcium) fly ash and combustion of sub-bituminous coal or lignite normally produces Class C (high calcium) fly ash. The chemical composition of fly ash generated by burning sub-bituminous coal is different from that generated by burning bituminous coal. The burning of sub-bituminous coal produces fly ash with calcium oxide content, in the range of 16 to 28%. But burning of bituminous coal generates a fly ash with CaO content in the range of 2 to 4%. According to ASTM C618, when the sum of Al_2O_3, SiO_2, and Fe_2O_3 is greater than 70%, the fly ash can be classified as Class F and when the sum is greater than 50% it can be classified as Class C fly ash [28].

Metal compound	Bituminous coal	Sub bituminous coal	Lignite coal
SiO_2	20-60%	40-60%	15-45%
Al_2O_3	5-35%	20-30%	10-25%
Fe_2O_3	10-40%	4-10%	4-15%
CaO	1-12%	5-30%	15-40%
MgO	0-5%	1-6%	3-10%
SO_3	0-4%	0-2%	0-10%
Na_2O	0-4%	0-2%	0-6%
K_2O	0-3%	0-4%	0-4%
LOI	0-15%	0-3%	0-5%

Table 1.3a Chemical compounds (% by weight) present in fly ash generated from different types of coal

1.3.1 Chemical Properties

The chemical properties of fly ash are influenced by the source of coal and the techniques used for storage, preparing and combustion. Coal consists of organic and inorganic substances. Organic matter is made up of and fixed carbon and volatile, mainly consists of carbon, oxygen and hydrogen. Fly ash is the residue generated from the combustion of inorganic matters, which is composed of silica, alumina and iron oxide, with smaller percentage of calcium oxide, sulphur oxide, magnesium oxide, unburned carbon and other compounds. Fly ash may be introduced in concrete as a cement containing fly ash or introduced as a separate component at the mixing stage.

Compounds	**Class C**	**Class F**
SiO_2	32.91	48.21
Al_2O_3	19.36	26.26
Fe_2O_3	5.38	10.61
$SiO_2+Al_2O_3+Fe_2O_3$	70.0	50.0
CaO (Lime)	28.85	2.66
MgO	4.83	1.14
SO_3	5.0	5.0
Loss on Ignition	0.64	7.79
Moisture Content	3.0	3.0
Insoluble residue	1.58	1.21
Na_2O	1.95	2.26

Table 1.3.1a Chemical Composition of Fly Ash

1.3.2 Physical properties

Fly ash consists of fine powdery particles that are spherical in shapes, either solid or hollow, and mostly glassy in nature. Bituminous coal fly ash particles are similar to that of a slit or fine sand. Subbituminous coal fly ashes are slit sized and slightly coarser than bituminous coal fly ash. One of the important parameters, that govern the use of fly ash for various applications, is lime reactivity. It has been found that lime reactivity of fly ash, which increases with its fineness. The strength of fly ash improves with time due to pozzolanic reactions. The pozzolanic reactivity of fly ash is influenced by the fineness, alumina content, silica LOI, and alkali content. Portland cement is manufactured with calcium oxide which is released in a free state during hydration. Some physical properties are:

1. Specific gravity of coal ashes lies in between 1.6 to 3.1[15]. Generally low value for the specific gravity of coal ash compared to ash fills, soils tent to result in low dry densities. The variation of specific gravity of the fly ash is the result of a combination of many factors such as gradation, particle shape and chemical composition. The reason for a low specific gravity could either the variation in the chemical composition or in particular iron content due to the presence of hollow cenospheres from which the entrapped air cannot be removed, or both.

2. Grain size distribution indicates that material is well graded, poorly graded fine or coarse and also helps in classifying the coal ashes. Based on the grain size distribution, the coal ashes can be classified as sandy silt to silty sand. Fly ash is silt sized nonplastic material. Poorly graded fly ash with coefficient of curvature ranging between 0.61 and 3.70.

3. Liquid limits and moisture density relationship**:** fly ashes have liquid water content ranging from 22to 64% for fly ash, and 45 to 104% for bottom ash. The liquid limit values exhibit by fly ash is not due to their plasticity characteristics but is due to their fabric and carbon content. Fly ash has a relatively low compact density, so reduce the applied loading and settlement of the supporting subgrade.

4. Compaction Behavior**:** the compacted unit weight of the materials depends on the amount and method of energy application, plasticity characteristics, grain size distribution and moisture content for fly ash. The tendency for fly ash is less sensitive to variation in moisture content than for soils. Fly ash has void content ranging between 5 to 15% at maximum dry density [15].

5. Strength behavior**:** the shear strength of fly ash is affected by the density and moisture content with maximum shear strength occurring at moisture content and the shear strength of fly ash samples is primarily from internal friction, however some apparent cohesion has been observed in bituminous fly ashes.

6. Hydraulic conductivity**:** the hydraulic conductivity of fly ash ranges from 10^{-4} to 10^{-6} cm/s, which is equivalent to the hydraulic conductivity of silty sand to silty clay soil. The hydraulic conductivity of fly ash is affected by grain size distribution, the degree of compaction, and internal pore structure. Since fly ash consists almost entirely of spherical shaped particles, the particles are able to pack during compaction, resulting in comparatively low hydraulic conductivity that minimizes the seepage of water through a fly ash embankment.

1.4 Brief Overview on Fly Ash Slurry

Slurry is essentially a mixture of solids and liquids. Abrasion, erosion, and corrosion are associated with pumping slurry that manufacturers of slurry pumps sometimes spend more money dealing with wear issues than with developing new hydraulics. Wear is very complex and too often oversimplified. It depends on many factors such as the hardness and shape of the crushed minerals, the microstructure of the surface of the pump part, the scaling of pipe and the speed of flow. Slurries can be classified into homogeneous and heterogeneous categories. Fine particles slurries exhibit homogeneous fluid behavior however mixture consists of two distinct phase exhibit heterogeneous behavior. Slurries generally deviate from Newtonian behavior and exhibit non-Newtonian characteristics. Many rheological models (Power’s Law, Bingham plastic Law, Yeild’s Law) have been developed for slurries and their behavior can be accurately predicted in laminar flow and sub-laminar flow. Heterogeneous slurries exhibit a more complicated flow behavior as compare to homogeneous slurries. These slurries are mixture of coarser particles in a homogeneous fluid.

1.5 Brief Overview on Additives/Surfactants

1.5.1 Surfactants/Additives

Surfactants can be cationic, anionic and non-ionic depending on the charge on head, the tail of additives consist of long chain of hydrocarbons, the difference in reactivity is created by the charge on the head. Studies indicate that in case of fly ash slurry, charged surfactant such as cationic and anionic are proven to be good in reduction of viscosity. Cationic surfactants work well with an organic counter ion. Non ionic polymer based surfactants increase the viscosity at buffer layer of slurry, this increase in viscosity is due to bending and twisting of polymer chain and this effect results drag reduction. After addition of polymer additive in the slurry the decrease in viscosity shows that the flow will become smooth due to reduction in wall friction.

1.5.2 Types of Surfactants

Anionic Surfactants are dissociated in water in an amphiphilic anion and a cation which is an alcaline metal or a quaternary ammonium. They are the most commonly used surfactants. They include alkylbenzene sulfonates, soaps, lauryl sulfate, di-alkyl sulfosuccinate, dispersants etc. Nonionic Surfactants do not ionize in aqueous solution, because their hydrophilic group is of a nondissociable type such as phenol, alcohol, ester, ether and amide. These nonionic surfactants are made of hydrophilic by the presence of a PEG chain, obtained by the polycondensation of ethylene oxide [29]. They are called polyethoxylated non-ionics. The polycondensation of propylene oxide produce a polyether which is hydrophobic in nature. Cationic Surfactants are dissociated in water into an amphiphilic an anion and cation. Cationic surfactants are more expensive than anionic surfactants because of the high pressure hydrogenation reaction to be carried out during their synthesis [29].

Sr. No.	Anionic Surfactants	Non-anionic Surfactants	Cationic Surfactants
1	Soaps and Other Carboxylates	Ethoxylated Linear Alcohols	Linear Alkyl-Amines
2	Sulfonation and Sulftation	Ethoxylated Alkyl Phenols	Alkyl-Ammoniums
3	Sulfates	Fatty acid esters	Amino-Acids
4	Sulfonates	Amine and Amide Derivatives	Alkanol-Amides
5	Organo phosphored	Alkylpolyglucosides	Oxy- and Ethoxy-Amines
6	Sarcosides or alcyl amino acids	Ethleneoxide/Propyleneoxide Copolymers	Amide-, Ester- and Ether-Amines

Table 1.5.2 Examples of different types of additives

1.6 Relevance of High Concentration Fly Ash Slurry Disposal System

Disposing of generated ash on landfill areas is an environmental friendly method to pumping ash slurries at high solids concentration. Slurry at high concentration has high viscosity forms a natural slope on the disposal area without the need for mechanical spreading and release minimum amount of water. This technology is referred as high concentrations slurry disposal system. For optimized design of slurry pipeline, an extensive database is necessary. Now -a-days most of the pipelines are designed based on some empirical relations developed over the years and are not always optimized design. The same is true for fly ash disposal pipelines being used in thermal power plants. Today, there are serious concerns raised about the environmental hazards of fly ash, there is an urgent need to take into the problem and adopt a methodology for transportation of fly ash at high concentrations.

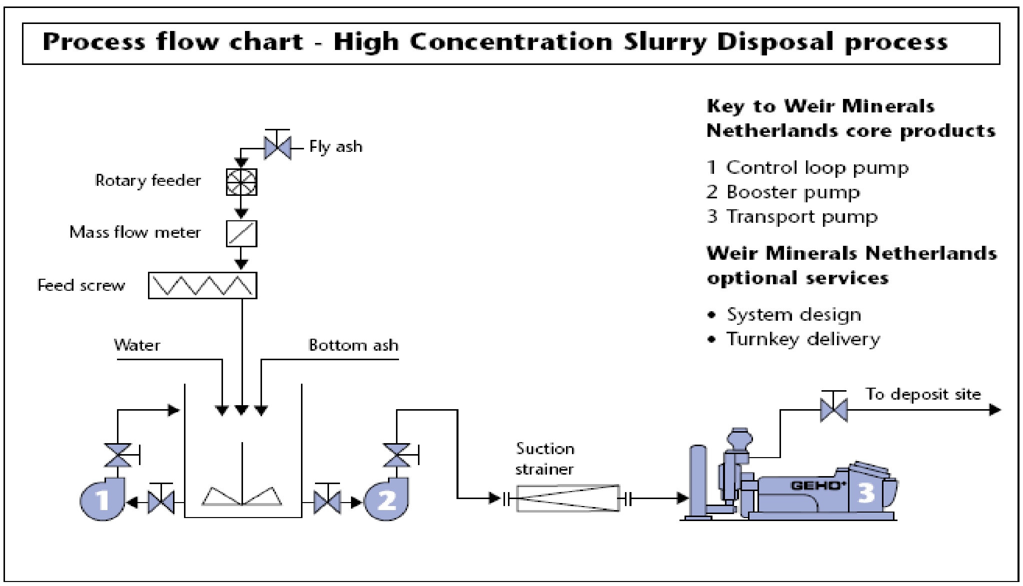

Figure 1.6a HCSP slurry disposal system

Disposal of fly ash through pipelines, the carrier fluid is water and it has to be tested for suitability so that fly ash does not react with water borne particles during transportation. The particle size distribution (PSD) and others properties such as coal quality, combustion efficiency is very essential to have a control over the top particles size since the operation of the pipeline depends critically on it. It is essential to measure the some rheological parameters before the ash disposal pipeline is designed. The head requirements for operating fly ash disposal pipelines at high concentration can be easily calculated using the rheological behavior of the slurry. It is possible to reduce the head requirements by using surfactants or additives which have dispersing as well as shear thinning effects. The economics of additives has to be established for each individual application. Most of the mineral industries use slurry pipelines for disposal of tailing and slime materials.

1.7 Rheological Models

Fluids that have a viscosity dependent on shear rate, such as complex fluids, exhibit non-Newtonian behavior. This behavior is difficult to describe with simple model. The description of two different fluids may require the use of two different rheological models. Complex fluids are modelized with classical rheological models like power law model or Bingham plastic and fluid behavior is defined with only two points of the rheological relation. These points correspond to higher shear rates. This approach can be justified in the case of complex fluids. The knowledge of rheological data and methods of predicting pressure losses are the key points to calculate pump rate and avoid any obstacle in complex slurries.

A fluid flow behavior deviates from the simple Newtonian, friction pressure loss equation become more complex and less accurate due to many assumptions. It is observed that one factor that may contribute to the inaccuracies in friction pressure loss calculation in complex fluid is the particular rheological model used in the development of a given theoretical expression or empirical correlation. One new rheological model that is thought to represent the flow behavior of complex fluids very well is the yield power law model or Herschel-Bulkley model. Yield power law model is the theoretical and practical aspects of Bingham and power law models. A fluid's rheological behavior is described according to the following equation (1)

$$\tau = \tau_0 + K.\gamma^n \qquad (1)$$

τ_0 = yield point, Pa

τ = shear stress, Pa

K = consistency index, Pa-s

γ = shear rate, s^{-1}

n = flow behavior index

The parameters K and n are similar to those of power law model. For fluids having a yield stress, the calculated values of K and n will be different from those calculated using power law model. The parameter τ_0 is the fluid's yield stress at zero shear rate.

The model is reduces to the power law rheological model when τ_0 =0 and reduce to the Bingham plastic model when n=1. Although power's law model is not accurate for very low shear rates, because data points on log-log plot are wider and linear regression line is not so accurate for these data points, the apparent viscosity values can be calculate from equation (2) as given below

$$\eta = K\gamma^{n-1} \tag{2}$$

CHAPTER 2

Literature Review

C. Sunil et al. (2010): investigated the pressure drop and rheological characteristics of fly ash and bottom ash slurry (4:1) at high concentrations (above Cw 50% by weight). Pressure drops were measured at various flow velocities using a pilot plant test loop at various concentrations in the range 50- 70% by weight. Rheological studies were carried out for mixture of fly ash and bottom ash slurry. By using the rheological data pressure drop has been predicted in a straight pipeline of 45 mm diameter at higher concentrations. They found that the pressure drop for any given solid concentration increases with increase in velocity and pressure drop increases with increase in solid concentration. The increase in pressure drop is higher in the low velocity range compared to high velocity region for any efflux concentration. They predicted that Bingham model is suitable for the Bingham plastic fluid flow such as mixture of fly ash and bottom ash (4:1) slurry at higher concentration and specific energy consumption decreases up to a concentration of 65% by weight and increases beyond this value [1].

Naik et al. (2009): examined that fly ash particles at higher concentration settle down quickly and can cause pipe jams and very high yield stress for starting the flow, this problem is conventionally solved by using lean slurries but then a large amount of water is wasted and also pumping power. Fly ash consists of metals like Fe, Al and alkaline earth materials increase drag effects which is related to specific energy consumption. Both these problems may be solved by adding certain additives and hence the main objective of the study is to keep the fly ash particles water borne while being transported and reducing drag friction. They studied the effect of drag reducing additive Cetyltrimethyl ammonium bromide (CTAB) with counter ion sodium salicylate (NaSal) on the rheology of fly ash slurries with solids concentration 40%. The shear range selected was 25-500s^{-1} and temperature range 20-40^{0}C. Physica MCR 101 Rheometer (Anton Parr Germany) with air bearing system having a co-axial concentric cylindrical cup and bob measuring system (cup dia. 28.9 mm, bob dia.26.7, measuring gap 1.1) was used for carrying out rheological measurements. The Zeta potential was measured by Zeta Sizer Nano series (Malvern instruments, U.K).They found that while the untreated fly ash slurry exhibited turbulent flow behavior with large yield stress and negative zeta potential value, in the presence of additive favorable conditions of shear thinning and zero yield stress were obtained for entire temperature range, the zeta potential values became positive which means that the suspension is more stable with additive. They claim that the ash slurry transported in this manner can save energy and allow the slurry transportation to take place at higher concentrations than conventionally used [6].

Manoj Sharma et al. (2012): for the reduction of solid waste through recycling of fly ash for oil well drilling operation fly ash was grinded and classified into several fractions using float and sink test which will help to improve the polydispersity of waste fly ash. Rheological studies were carried using waste fly ash with varying particle size, particle size distribution and percent solid loading using Fann rotational viscometer. Wall shear rates and shear stresses were calculated using Fann viscometer readings. Predicted wall shear rate and shear stress are used to calculate Herschel-Bulkley rheological model parameters for finding the shear rate dependent viscosities. They observed that smaller particle size distribution or narrow particle distribution and increased solid loading of classified fly ash will improve the suspension viscosity and will help to manipulate the rheological behavior of the suspensions for efficient utilization. They compared the rheological results of fly ash suspensions with aqueous bentonite clay suspensions to test the suitability of waste fly ash for oil well drilling application. They concluded that bentonite suspensions exhibits high share rate of deformation than the fly ash suspension particularly at high shear stress [24].

Kamal EI-nahhas et al. (2009): observed that horizontal flow depends upon gravitational velocity, the turbulence within the liquid the carrier properties and particle-particle interaction. An open-loop recirculation pipeline system was used for testing the slurry flow behavior. Inductive differential pressure transducers were used to measure the pressure losses between the pressure tappings. The digital data signal to a computer, which is accessed with MATLAB software that enables for online supervisory, analysis and data acquisition. These data are input to the computer software for processing to present the supervisory plots online during the operations. All pressure transducers had been calibrated periodically against the standard device, U-tube manometers. For the tested sand slurries the relative solids effact the flow velocity indicating the beginning of solids bed formation in the pipe. They investigated that for the same solids throughout as the solids concentration increases the specific energy consumption decreases and hydrotransport of dense slurry could be more efficient and economic [4].

Carmel et al. (2009): used the anionic surfactants n-alkyl sulphates, n-alkylcarboxylates, n-alkylsulphonates with hydrocarbon chain between $C_{7\ \mathrm{and}}$ C_{12}. Pastes were prepared, followed by intense mixing stirring at room temperature during 2 min using a kitchen mixer. The total volume of air entrained in pastes was determined by density measurements. To determine the extent of surfactant adsorption or precipitation in the cementations pastes, the amount of surfactant available in the paste solution was measured chemical oxygen demand. They investigated that surfactants activity and air-entraiment effectiveness should be highest for n-alkylsulphates bearing the longest hydrocarbon chain, namely n-$C_{12}SO_4$ and cement and FA- cement pastes influence the cement composition and cement fluidity [7].

Vadpalli et al. (2007): the fly ash from South African power stations were used to treat acid mine drainage and the insoluble residuals solids that were obtained as a result of the reaction between fly ash and acid mine drainage proved suitable as a backfill materials for mine stabilization. Particle size distribution of FA varied from time to time depending on burning conditions in the power station. It is found that all the slurries recovered from the flow curves by fitting the Harschel-Bulkley model to the experimental data. They investigated that the particle size distribution (PSD) influences the reactive surface area and concomitantly increased the slurry viscosity [5].

Van der M. Merwe et al. (2011): South African fly ash sample were tested under a variety of conditions with an anionic surfactant, sodium lauryl sulfate to modify the surface and physical properties of fly ash. The anionic surfactant SLS with a purity of 98% was obtained from Merck. X-ray powder diffraction analyses were carried out on

X' Celerator detector and variable divergence and receiving slits with Fe filtered Cu Ka radiation. A JSM 840 Scanning Electron Microscope (SEM), Operated at 5 KV, was used to view the samples of fly ash. It is evident that further investigation need to be performed in order to fully understand the interaction between fly ash and SLS [8].

Bournoville et al. (2002): the effect of concentration, yield stress and hydrodynamic interactions on Rheology of non-Newtonian suspensions of two different water-washed municipal solid waste (MSW) incinerator fly ashes. A thixotropic and shear-thinning behavior is observed for aqueous suspensions of non-treated fly ashes. They concluded that the viscosity is sensitive to the concentration of solids [2].

Senapati P.K et al. (2010): a model incorporating maximum solids fraction (Φ), power law index (n), median particle size (d_{50}), co-efficient of uniformity (C_u), shear rate (γ) has been developed to predict the viscosity of slurry which is highly pseudo-plastic & whose behavior can be described by a non-Newtonian power law model in the range of solids concentration. Prediction of Φ has been determined directly from rheological data measured experimentally in a realistic system which is 0.62 in value. Five flyash samples were obtained from the captive power plant of NALCO located at Angul Orissa. The particle size distribution was determined using Malvern make laser particle size analyzer, Morphological studies of 2 ash samples were undertaken using a Joel Super Probe (JXA - 8100). The elemental analyzer of the bulk ash samples was carried out by Philips PW2440X-ray spectrometer. Shear thinning behavior for all the samples at higher solids volume fractions in the range 0.32 to 0.49. Proposed model helped to access the motion of solid particles in a non-Newtonian flow regime [3].

Shunsuke Hashimoto et al. (2012): the hydrate structure mainly depends on the size, shape, and physical properties of enclathrated guest species. The hydrate formed from tetra-*n*-butyl ammonium salt solution has been known as a semi-clathrate hydrate where the quaternary ammonium cation and anion are incorporated with the hydrogen bonds of water molecules to construct hydrate cages. Tetra-*n*-butyl ammonium bromide hydrate is well known as a semi-clathrate hydrate former. The concentration of aqueous TBAB solutions results in differences of the crystal structure and thermodynamic stability of TBAB hydrate. The viscosity characteristics of TBAB solution and hydrate slurry under various temperature conditions were measured by use of stress-control-type Rheometer. The zeta potential of the TBAB hydrate particles in their slurry was measured by use of zeta potantializer. The apparent viscosity of TBAB solution increases gradually in the range of > 500 s-1. It is generally considered that TBAB behaves like a cationic surfactant in aqueous solution. The behavior of TBAB hydrate slurry in tube or duct is macroscopically and industrially important. The apparent viscosity of TBAB hydrate slurry increases with the temperature decrease which is derived from the increase of hydrate fraction (from 0.12 to 0.25). The apparent viscosity of TBAB hydrate slurry also increases as the concentration of TBAB in aqueous solution becomes higher, where the hydrate fraction increases. The viscosity increase with temperature decrease is mainly derived from the increase of hydrate fraction. The surfactant-concentration dependence of the apparent viscosity of TBAB hydrate slurry prepared from 20 wt% aqueous solution the zeta potential of the TBAB hydrate slurry was measured by use of zeta. It is concluded that addition of minute cationic-surfactant reduces the apparent viscosity of TBAB hydrate slurry drastically and also the apparent viscosity of TBAB hydrate slurry increases as the hydrate fraction increases [9].

Seshadri et al. (2008): studied the effect of additive (sodium hexameta-phosphate) on head loss in the high concentration slurry disposal of fly ash, they took five slurry samples of fly ash having different highest particle size and particle size distribution (PSD) for determining the rheological behavior at different concentrations. Then the effect of the additive they studied. Based on rheological data the pressure drop has been predicted at different concentrations with and without additive. They observed that the pressure drop for any concentration increases with the increase Reynolds number for same particle size. They noted that for given particle size and concentration at any selected velocity there is a significant reduction in pressure drop. It was observed that pressure drop increases with increase in concentration [10].

C. Sunil et al. (2009): An attempt to establish the relationship between the settled solid profile in ash pond and the physical/ rheological properties of coal ash slurry at high concentration was made to evaluate some characteristics of slurry which favour (HCSD) high concentration slurry disposal system. A hopper shaped mixing tank made form 3 mm thick GI sheet was placed on a flat base of FI tray, plug type valve (Make: AUDCO) was used for the flow of slurry from top. Experiment on FA: BA (4:1) slurry at higher concentration 60%, 65% & 70% (by weight) was done to determine angle of repose of the settled solids. The cone angle was measured for both impervious & pervious beds. For making pervious bed, dry fly ash was used & it was spread evenly over the whole tray to height of 4 cm. High values of yield stress & Bingham viscosity of the slurry result in higher cone angle of the deposited slurry. Cone angle increases with increase in solid concentration for FA slurry as well as mixture of FA & BA slurry but its values are lower [11].

Usui et al. (2001): predicted that sphericity of fly ash particles is measure by different particle size ranges by means of microscopic CCD camera and automatic particle image processor. The apparent viscosity of fly ash-water slurries was measured by a remoter (Iwamoto Seisakusho Co., Ltd. Model IR-200) with coaxial rotating cylinders. The particle diameter determined by laser diffraction method is interpreted as the volume based diameter and the circularity of the two dimensional trajectory image of a particle is conventionally determined by an image processing instrument (analyzer, FPIA-2000, Sysmex Co). Simha’s cell model was used to predict the completely dispersed suspension for given solid volume fraction, particle size distribution and maximum packing volume fraction. They investigated that maximum packing volume fraction for non-spherical suspension is successfully used to predict the slurry viscosity under completely dispersed conditions [23].

F. Hadri et al. (2011): studied that temperature and concentration effect on the drag reduction in the pipes. They investigated that an aqueous solution of cetyltrimethyl ammonium chloride and sodium salicylate with a concentration lower than 100ppm reduce drag and found out that the maximum drag reduction rate is obtained at Reynolds numbers higher than 45,000 for the concentration of 150ppm and around 11,000 for the concentration of 25 ppm. At low concentration (25 ppm) the drag reduction occurs at low Reynolds numbers, the maximum of drag reduction reaches 60% the critical Reynolds numbers Onset Reynolds number (ORN) and the Retro-onset Reynolds number (RORN) are coincident. They concluded that at higher concentrations (150 ppm), the drag reduction rate, the efficient interval and the second Reynolds numbers (RORN) increase. The drag reduction rate exceeds 78% between 25 and 50 ppm, the RORN (corresponding to the fall of the drag reduction) changes rapidly (10,000–30,000). From 50 and 75 ppm, the RORN changes more slowly (30,000–43,000). And from 75 to 150ppm the RORN evolution is rather low (43,000–48,000). At temperatures higher than 10 ◦C, the friction factors tend to reach the Virk's asymptote and follow it. At temperature higher than 40 ◦C the interval of DR efficiency is prolonged towards the lower Reynolds numbers. For higher Reynolds numbers the Virk's asymptote is nearly reached. A critical temperature (CT) exists for all concentrations, above which the DR disappears. This temperature increases with the concentration. As mentioned before, for 25 ppm, 25 °C is obtained; this temperature reaches 40 °C for 50 and 75 ppm [22].

R. Bhattacharjee et al. (2010): concluded that fly ash based geopolymer concrete follows Bingham equation with a very good accuracy. They used the mixture of sodium hydroxide and sodium silicate solution as alkali activators Fly ash based geopolymer concrete mixes with were tested with a rate controlled concrete rheometer to study the rheological behavior. The down curve shows a linear relationship between toque and rotational frequency and follows Bingham equation. Rheological parameters in terms of yield stress and plastic viscosity can be estimated from the down curve of torque-speed plot [19].

D. P. Bentz et al. (2010): used the high volume fly ash (HVFA) mixtures and Portland cement to study the rheology behavior. These mixtures are being used more and more in practice, but a common remark from contractors is that HVFA mixtures can be susceptible to long delays in finishing and sometimes lack necessary early age strength development. The complexity of the cement, admixture and fly as interactions that contribute to excessive retardation is recognized by laboratory and field personnel, with these interactions being further dependent of environmental conditions and inherent material variability. Cement pastes were prepared with a water-to-cementitious materials or water-to-binder ratio by mass of 0.30. High shear follow the procedure developed by the Portland Cement Association. For a given mixture, all powder materials were pre-blended for 30 min in a sealed plastic jar on a Turbula1 blender. The high range water reducing agent (HRWRA) was premixed with the mixing water. Rheology measurements were conducted using the stress growth method. This method shears the paste at a shear rate of 0.1 s^{-1} (the lowest possible rate with the rheometer employed) and the shear stress is measured versus time. The shear stress increases linearly until the sample yields and starts to flow. Isothermal calorimetry was conducted for a period of at least 7 d using single or replicate paste specimens have mass of 5 to 6 g. The prepared paste was first placed in the glass calorimeter vials then the vials were sealed and the sealed vials were then loaded into the calorimeter along with a reference vial containing only cement powder. Finally they concluded that rheology and ASTM C191 setting time measurements have confirmed that additions of either calcium hydroxide powder (5%) or rapid set cement (5–10%) can significantly reduce the setting time for HVFA mixtures that have exhibited excessive retardation [18].

L. Li et al. (2013): used the additives rhamsan gums, carboxym ethyl cellulose and xanthan gum and Usui’s thixotropy model to find the relationship between flow rate and pressure drop. They concluded that the viscosity of fly ash–water slurry increases as the concentration of stabilizing additive increases and the concentrations of stabilizing additives to give the same viscosity as untreated slurry at 0.2 wt%, 0.45 wt%, and 0.3 wt% and also concluded that the apparent viscosity of slurry without additive rapidly increases as the fly ash concentration exceeds 71.5 wt%. Finally they found out the result that stabilizing additives are effective in increasing stability of fly ash–water slurry and the plant transportation costs of dense slurry transportation with additive feeding system are higher than the costs without additive feeding system [16].

Anoop et al. (2009): studied the rheological properties of alumina-water nanofluid, which are electrostatically stabilized and the increase in suspension viscosity due to presence of this electrical double layer causing additional electroviscous effects. Based on dynamic light scattering studies particle agglomeration and its subsequent effect on the viscosity of alumina-ethylene glycol nanofluid, where electroviscous effects are absent. They noted that the understanding of electroviscous effect is equally important as understanding the particle agglomeration effect and understanding both the effects is central to revealing the physics of nanofluid rheology. They observed that the electroviscous effects caused by stabilization procedure are important and can influence viscosity increase for waterbased nanofluids. Finally they concluded that Newtonian behavior is exhibited for both water-based and ethylene glycol-based nanofluids for the particle concentration between 0.5–6 vol. [25].

S. K. Mishra et al. (2002): Studied the rheological behavior of some Indian coal-water slurry (CWS) using a HAAKE RV30 viscometer. They observed that solid concentration, ash content, pH and temperature effect on the rheology of CWS. They also observed that the slurries prepared in this study exhibit pseudoplastic behavior and CWS became more viscous with increases in ash content and solid concentration. They concluded from the study that apparent activation energy independent on the rate of shear and solid concentration and apparent viscosity is high in acidic medium. CWS shows non-Newtonian behavior at low pH [17].

CHAPTER 3

EXPERIMENTAL WORK

3.1 Additives Used

Four types of additives of different nature are used to study the rheological behavior of fly ash slurry at higher concentrations (above 40%). The physical and chemical properties of used additives are given below. After studying the properties of these additives following 4 additives are select for experimental work.

- ❖ Detergent Ariel (Anionic Surfactant)
- ❖ Glycerol (Non-ionic Surfactant)
- ❖ Polyethylene Glycol (reffered as PEG)
- ❖ Sodium Lauryl Sulfate (reffered as SLS)

A brief description of these additives are given below

3.1.1 Detergent Ariel

Ariel acts as an anionic in nature. It is made by Procter & Gamble. Ariel first appeared on the UK market in 1967 and was the first detergent with stain-removing enzymes. With the rise in popularity of automatic front-loading washing machines, a suitable low-suds variant was launched in the early 1970s. The mid-eighties saw the range expanding to encompass liquid detergent and compact powder. It is the flagship brand in Japan, Europe, Mexican, Braziliane, Peruvia, Turkish, Filipino, Indian, Colombia, Chilean and Venezuelan.

S.NO.	Parameters	Value
1	CAS	64425-86-1
2	pH (10% aqueous solution)	9-11
3	Specific gravity	0.525
4	Reserve alkalinity	8.96
5	Physical state	Solid granules
6	Odour	Scented and /or scented
7	Citric acid	1-5%
8	Disodium disilicate	1-5%
9	Sodium carbonate	10-20%
10	Sodium carbonate peroxide	10-20%
11	Sulfuric acid	1-5%
12	Benzenesulfonic acid	5-10%
13	Water solubility	high
10	Cost per 1000 gm	191.07/-
11	Manufactured by	Procter &Gamble,KT130KP,UK

Table3.1.1a Physical and Chemical properties of detergent Ariel

3.12 Polyethylene Glycol

Polyethylene glycol is produced by the interaction of ethylene oxide with water, ethylene glycol, or ethylene glycol oligomers. It is coupled to hydrophobic molecules to produce non-ionic surfactants. The reaction is catalyzed by acidic or basic catalysts. Ethylene glycol and its oligomers are preferable as a starting instead of water, because they allow the creation of polymer with a low polydispersity.

HO-CH2-(CH2-O-CH2-)n-CH2-OH

Figure 3.1.2 a Chemical structure of PEG

S.NO.	Parameters	Value
1	CAS	25322-68-3
2	Molar mass	20,000 g mol^{-1}
3	Molecular formula	$C_{2n}H_{4n+2}O_{n+1}$
4	Minimum Assay activity	97%
5	Flash Point	182-287 °C
6	Soluble	water
7	INS	E1521
8	Cost per 100 gm	130 /-
9	Manufactured by	Dow Chemicals

Table 3.12 b Physical and Chemical properties of PEG

3.1.3 Sodium Lauryl Sulfate

Sodium lauryl sulfate or sodium ether sulfate (SLES) is a detergent and surfactant found in many personal care products (soaps, shampoos, toothpaste etc.) SLES is an inexpensive and very effective foaming agent. SLES, SLS and ALS are surfactants that are used in many cosmetic products for their cleansing and emulsifying properties. They behave similarly to soap.

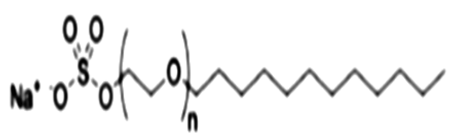

Figure 3.1.3 a Chemical structure of SLS

S.NO.	Parameters	Value
1	CAS	9004-82-4
2	Molecular Weight (M.W.)	420 g/mol^{-1}
3	Molecular formula	$CH_3(CH_2)_{10}CH_2(OCHCH_2)_nOSO_3Na$
4	Minimum Assay activity	99 %
5	Heavy metals	0.0002 %
6	Phosphate (PO_4)	0.0001 %
7	Chloride (Cl)	0.03 %
14	Cost per 100 gm	268/-
15	Manufactured by	Loba Chemie, Pvt. Ltd. Mumbai 400 005, India

Table 3.13 b Physical and Chemical properties of SLS including cost

3.1.4 Glycerol

Glycerol is a simple polyol compound. It is colorless, odorless, viscous liquid that is widely used in pharmaceutical formulations. Glycerol has three hydroxyl groups that are responsible for its solubility in water and its hygroscopic nature. The glycerol backbone is central to all lipids known as triglycerides. Glycerol is sweet-tasting and of low toxicity.

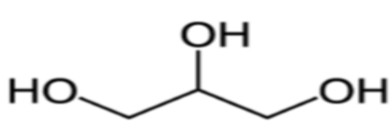

Figure 3.14 a Chemical Structure of Glycerol

S.NO.	Parameters	Value
1	CAS	56-81-5
2	Molar mass	92.09 g mol^{-1}
3	Molecular formula	$C_3H_8O_3$
4	Sulfated ash	0.01 %
5	Water	9 %
6	Heavy metals	0.0005 %
7	Ammonium (NH_4)	0.0005 %
8	Aldehyde	0.001 %
9	Chloride (Cl)	0.001 %
10	Sulphate (SO_4)	0.001 %
11	Density	1.261 g/cm^3
12	Melting point	17.8 °C
13	Boiling point	290 °C
14	Refractive index	1.4746
15	Viscosity	1.412 Pa-sec
16	Flash Point	176 °C
17	Cost of 500ml	378/-
18	Manufactured by	Loba Chemie Pvt. Ltd.107 Wodehouse Road (Mumbai)-400 005

Table 3.1.4 a Physical and Chemical properties of Glycerol

3.2 Fly Ash Used

3.2.1 SEM analysis of fly ash

Image obtained from scanning electron microscope (SEM) is shown in figure 3.2.1a. It may be observed that they appear as plain spherical particles of varying diameters. The surface of fly ash particles appears smooth and clean. A scanning electron microscope (SEM) is a type of electron microscope that produces images of a sample by scanning it with a focused beam of electrons. The electrons interact with atoms in the sample, producing various signals that can be detected and that contain information about the sample's surface topography and composition. The electron beam is generally scanned in a raster scan pattern, and the beam's position is combined with the detected signal to produce an image. SEM can achieve resolution better than 1 nanometer. Specimens can be observed in high vacuum, low vacuum and in environmental SEM specimens can be observed in wet conditions.

3.2.2 Particle size distribution (PSD) of fly ash

The variation in the size of the particles in the solid sample and the percentage of particles present in different pre-selected size ranges are determined to establish the particle size distribution (PSD). Three methods namely sieve analysis, hydrometer analysis and laser diffraction is employed to get this distribution. PSD of fly is estimated using the process of mechanical sieving. In this process sieves are arranged from top to bottom, with topmost sieve having mesh width of maximum size. Sizes in sieve are measured in micro meter. There are basically two standards to designate a sieve; these are British and American standards. In both these standard a given sieve is designated with a number called mesh number. A conversion table between British and American standard is given in Annexure E. The sieves used for this experiment are designated with British standard.

Figure 3.2.2 (a) Fly ash sample (b) Sieve system arrangement (c) Mechanical sieving machine

Procedure

- 200 grams of fly ash sample is dried in an oven at 175°C for 35 minutes to remove the moisture content.
- After removing the moisture content the sample put on the topmost sieve No.8 and arranged them in decreasing micrometer range of sieve. put the all sieves on the sieve shaker and tightly these with metal bin.
- After that timer is set for 15-20 minutes of sieving time.
- Measuring the weight of fly ash collected in each sieve and checks the particle size distribution of fly ash.

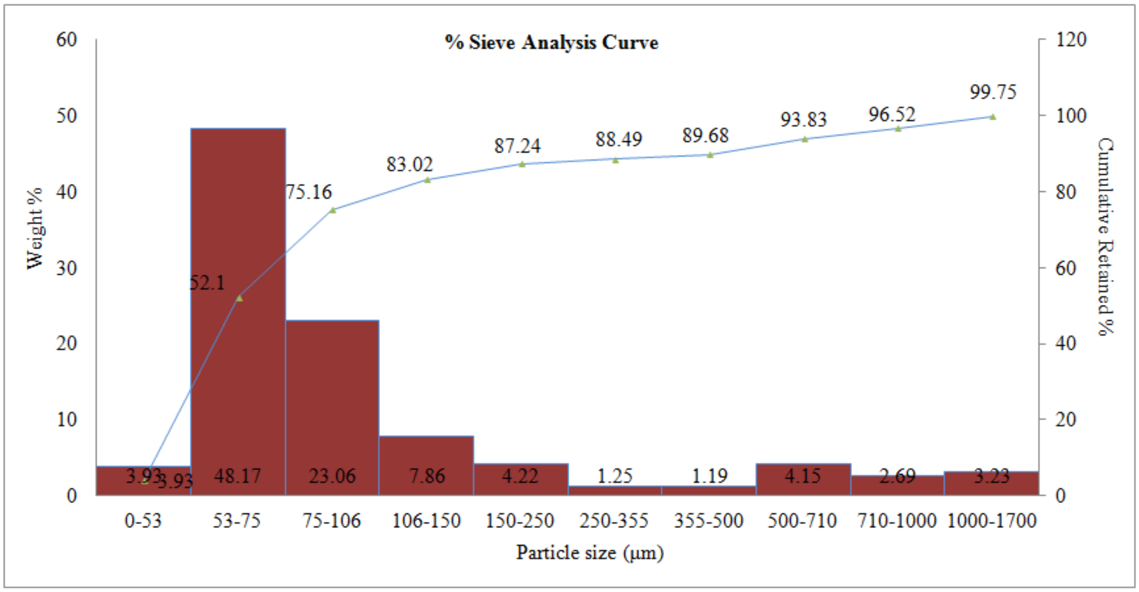

Figure 3.2.2d Particle size distribution of fly ash with curve for cumulative weight retained

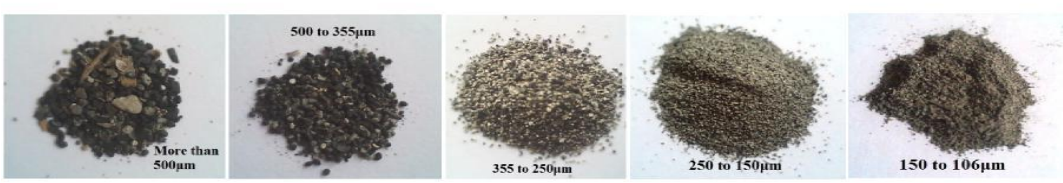

Figure 3.2.2e Visuals of particle greater than 100 µm

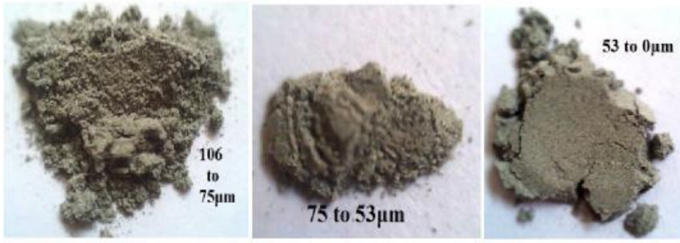

Figure 3.3.2f Visuals of particle size less than 100 μm

It can be observed that majority of fly ash particles (about 50%) lie in the range of 53 to 75 μm, 24% lie from 75 to 106 μm range and about 8% lie in 106 to 150 μm range. From cumulative retained graph we can observe that these 3 particle ranges cover about 82 % of the total weight. It will be analysed in the upcoming results that the overall viscosity of fly ash slurry depends mainly on these 3 particle ranges. It will also be observed that presence of large particles (size more than 100 μm) affects the flow properties adversely by increasing viscosity. But due to their smaller percentage smooth flow is maintained.

3.3 Instrument Used

3.3.1 Rheolab QC (Make: Anton paar)

Rheolab QC is a quality control rheometer based on state-of-the-art technologies also used in R& D rheometer. It combines unrivaled performance with easy operation and robust design. From quick single-point checks over flow curve and yield point determinations to complex rheological investigations: Rheolab QC sets new standards for carrying out routine rheological tests. The EC motor technique, the low friction bearing and the patented normal force sensor have been optimized over years to satisfy the highest demands of rheologists. This powerful rheometer is an excellent example of a modern measuring instrument utilizing all available technical possibilities to ensure flexible, reliable and simple operation. The innovative and patented features Toolmaster™ and TruGap™ are breakthroughs in terms of user-friendliness

 

3.3.2 Technical features

Some Techanical highlights are as follows

- Powerful, highly dynamic EC motor drive
- Connection to printer and bar code reader
- Real-time position control oscillation (DSO): Fast and accurate strain control
- Wide speed and torque range
- Controlled shear rate (CR) and controlled shear stress (CS) test settings
- Stand-alone and software controlled operation
- Wide range of measuring systems for all kinds of applications
- Ethernet connection for remote control of the instrument through the company network
- Downloadable measuring profiles and data retrieval for stand-alone systems
- Nano rheology for nonmaterial science

3.3.3 Detailed specifications

Property	Range
R.P.M	$0.01 min^{-1}$ to $1200 min^{-1}$
Viscosity range	1 to 10^9 m Pa-s
Shear rate	10^{-2} to $4000 s^{-1}$
Shear stress	0.5 to 3 x 10^4 Pa
Torque	0.25 m-Nm to 75m-Nm
(depending on geometry used)	
Angular resolution	2 μ rad
Temperature range	-20°C to 180°C
Physical variable (measurement and evaluation)	• Shear rate • Shear stress • Dynamic viscosity • Yield Stress • Torque • Temperature • Compliance • Kinematic Viscosity • Deformation • Time

Table 3.3.3d Specifications of Rheolab QC rheometer

3.4 Preparation of slurry for rheometer

3.4.1 Preparation of slurry without additive

All the samples of fly ash slurry are prepared by weight. The required concentration of fly ash is weighed on a weighing scale as shown in figure 3.4.1.1a with accuracy of 0.001 gram, water as a solvent is measured in millimeters (ml), and its concentration is calculated by subtracting the % conc. of fly ash from 100. Required solution is mixed thoroughly for 15-20 minutes for homogenous mixing and then put this slurry into the cylindrical bob of the rheometer. Then attach the bob to the magnetic coupling of rheometer for experiment.

3.4.2 Preparation of slurry with additive

All the Samples are prepared by weight (Cw). The required concentration of fly ash is weighted, and concentration of water is calculated same as before, the weight of additive is measured on weight scale with accuracy of 0.001 gram. The weight is calculated based on the percentage concentration of total solution. These concentrations of fly ash and additive are mixed thoroughly with water for 15-20 minutes for proper mixing. The slurry obtained is immediately poured into the cylindrical bob and then connected with rheometer for measurement.

CHAPTER 4

RESULTS AND DISCUSSIONS

4.1 Study of Flow Behavior of slurry at Higher Fly Ash Concentration

4.1.1 Effect on viscosity on slurry at higher concentration

In this experiment, concentration of fly ash is varied from 40% to 65% by weight and the effect on viscosity of slurry with each concentration is studied for a range (0 to 400s^{-1}) of shear rate. The shear stresses vs shear rate graphs are shown in figures (4.1.a to 4.1.1 d).it can be observed that at high concentrations the flows shows Non-Newtonian behavior or shear thinning behavior.

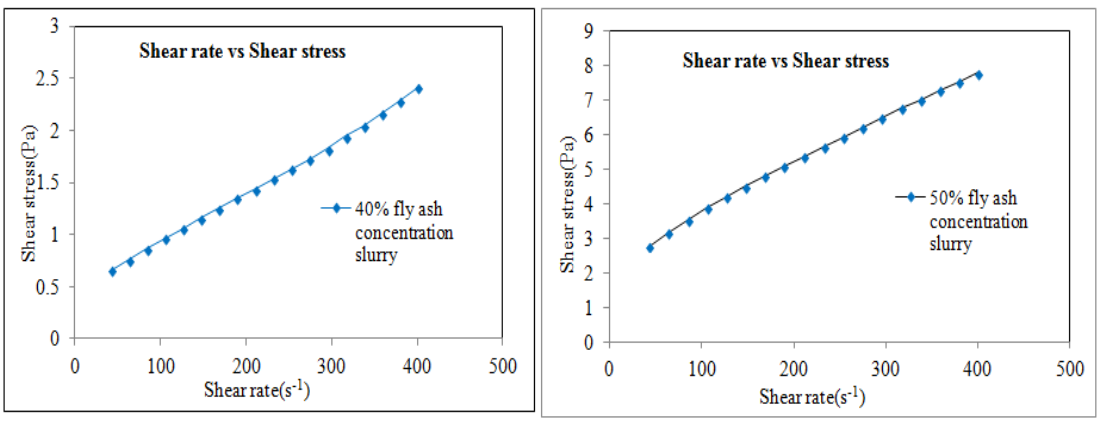

Figure 4.1.1 (a) System generated shear stress graph at 40% fly ash (b) at 50% fly ash

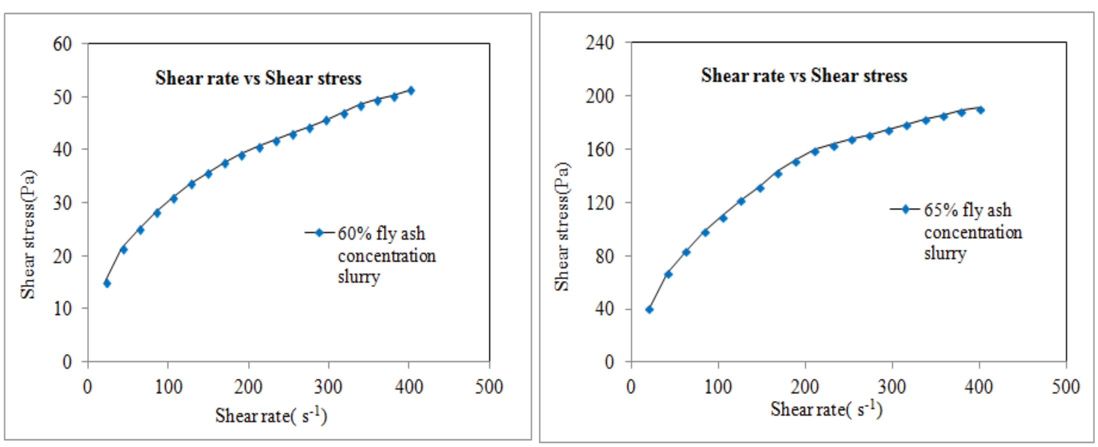

Figure 4.1.1 (c) System generated graph at 60% fly ash (d) at 65 % fly ash

Measurement data is listed in Annexure A

4.1.2 Comparison of shear stresses and viscosities between shear rates at different concentration

Figure 4.1.2a and figure 4.1.2b compare the shear stresses and viscosities of slurries at different concentrations. It can be observed that shear stresses increased drastically with increase in fly ash concentration an also observed that viscosity at 65% concentration is very large as compare to 40% concentration. This increase in viscosity shows that slurry become dense from leaner mixture.

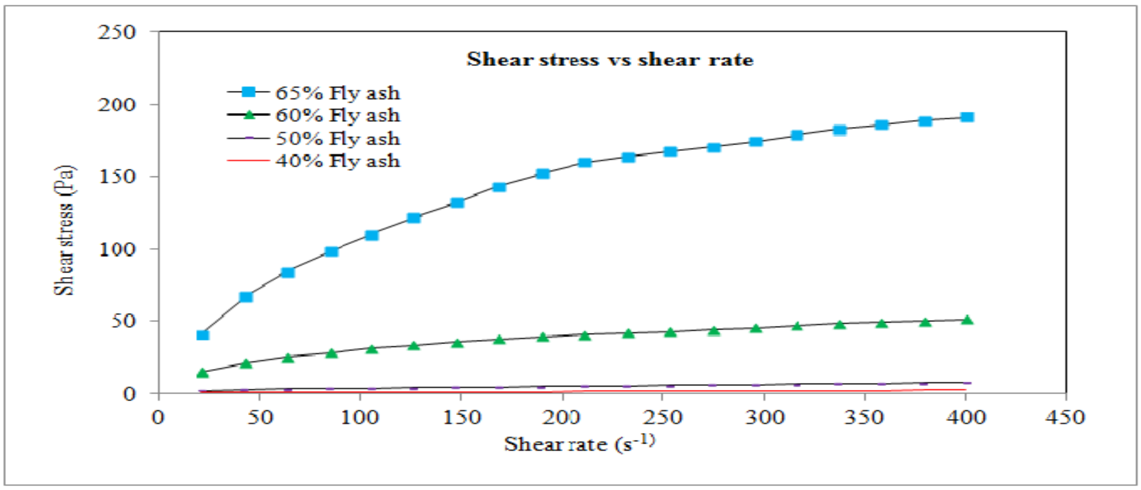

Figure 4.1.2 (a) Comparison of shear stresses of different concentration slurries

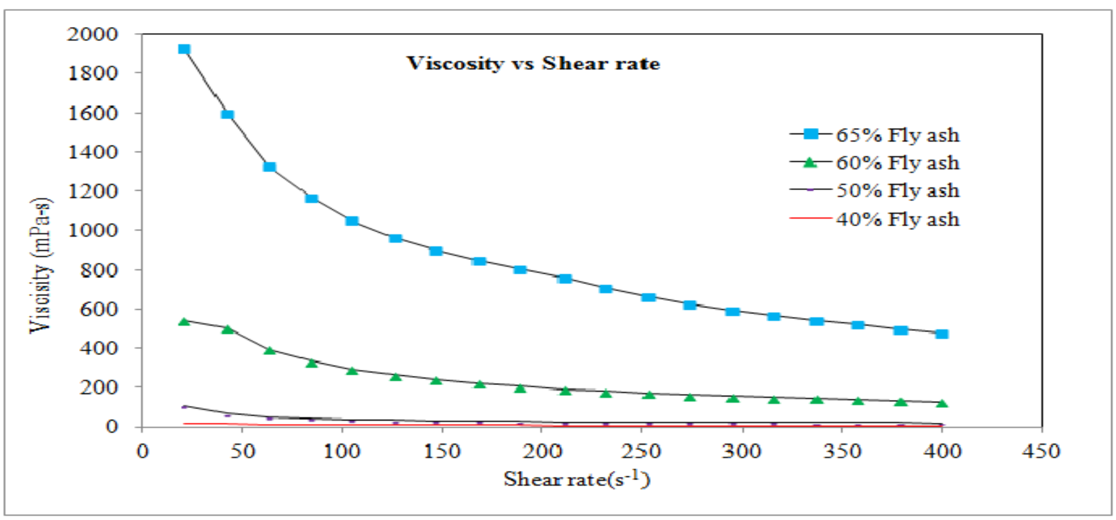

Figure 4.1.2 (b) Comparison of viscosities at different concentration slurries

4.1.3. Modelling using Power's Law rheological model

From figure 4.1.3b it is observed that even at high concentrations of fly ash in slurry (such as 40%, 50%, 60% and 65%) the apparent viscosity points still represents approximately a straight line. This indicates that viscosity lines are straight so there is a possibility that shear stress curve can be approximated using a power law model. In this section, Power's model is used to calculate values of apparent viscosities. To find the applicability of this model is to plot the shear stress vs shear strain values on logarithmic scale as shown in figure 4.1.3a and observe weather these points together form a straight line or not. It can be observed that line are straight on log-log plot with good coefficient of regression 'r'.

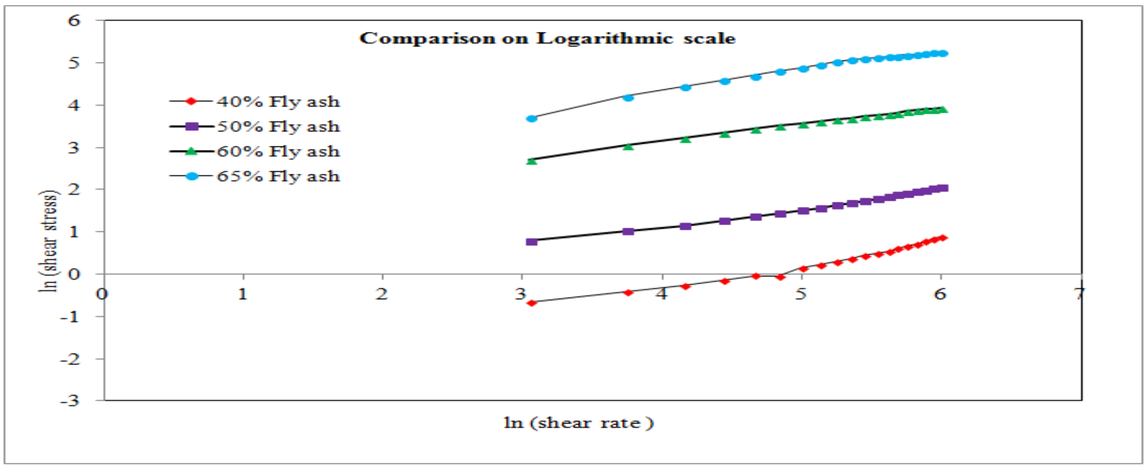

Figure 4.1.3a Comparison of shear stress vs shear strain on logarithmic scale

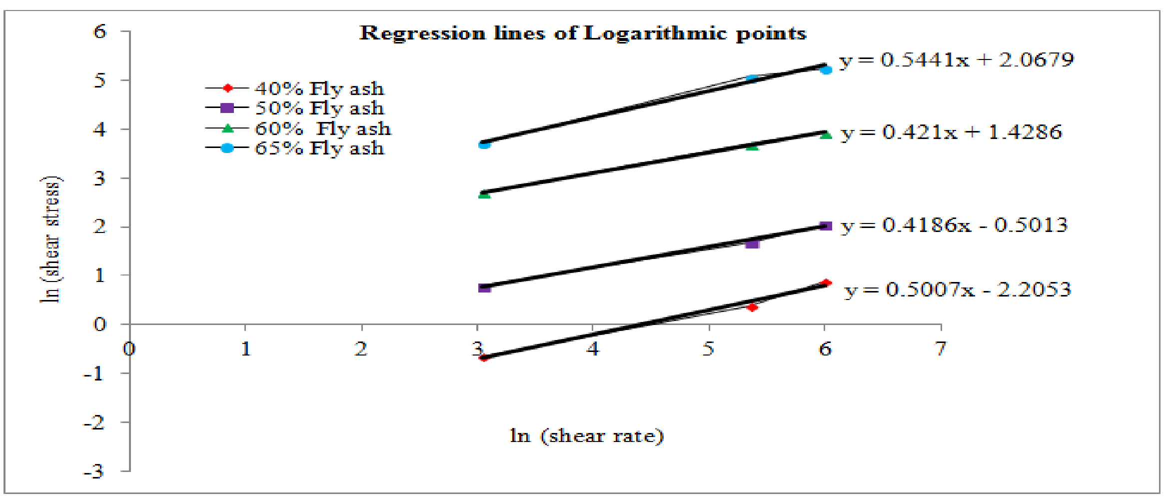

Figure 4.1.3b Regression lines with points plotted in the range of one standard deviation

Coefficient of Correlation r			
r1(40% fly ash)	r2 (50% fly ash)	r3 (60% fly ash)	r4 (65% fly ash)
0.9308	0.9526	0.9977	0.9967

4.1.3b Regression lines with points plotted in the range of one standard deviation

Slope (n) of Regression Lines			
40% fly ash	50% fly ash	60% fly ash	65% fly ash
n= 0.5007	n= 0.4186	n= 0.421	n= 0.5441
ln(K)= -2.2053 K= 0.1102	ln(K)= -0.5013 K= 0.6057	ln(K)= 1.4286 K= 4.1728	ln(K)= 2.0679 K= 7.9081

Table 4.1.3c Table showing the modeling parameters calculated using experimental data

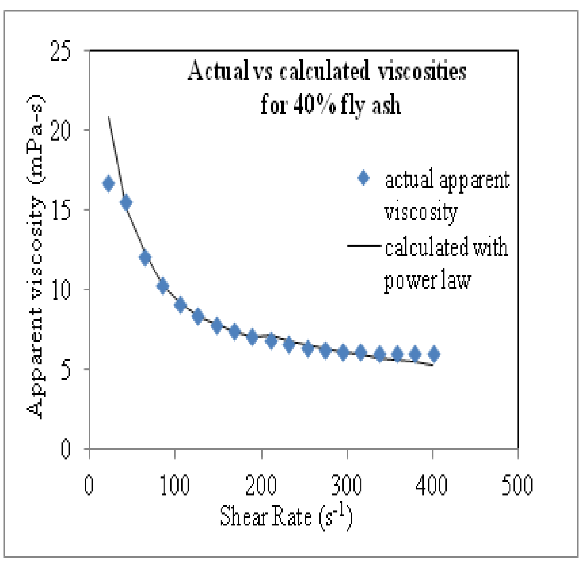

Figure 4.1.3d 40% fly ash slurry

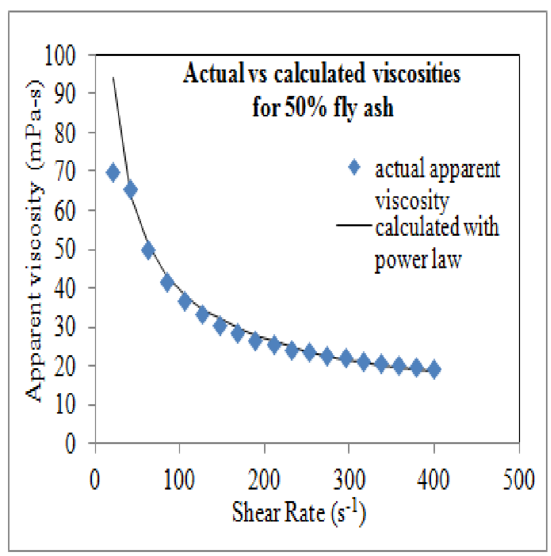

Figure 4.1.3e 50% fly ash slurry

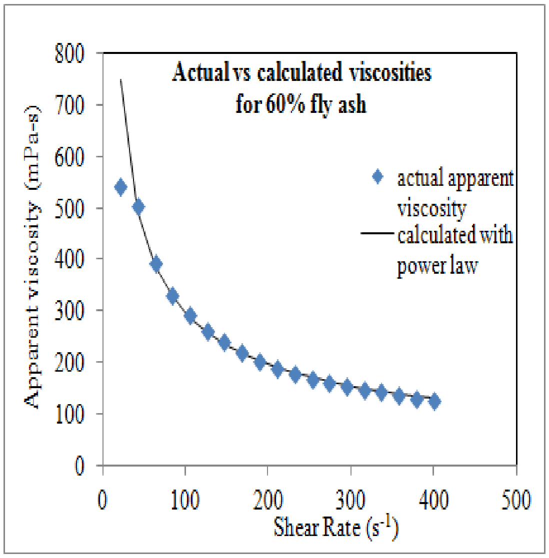

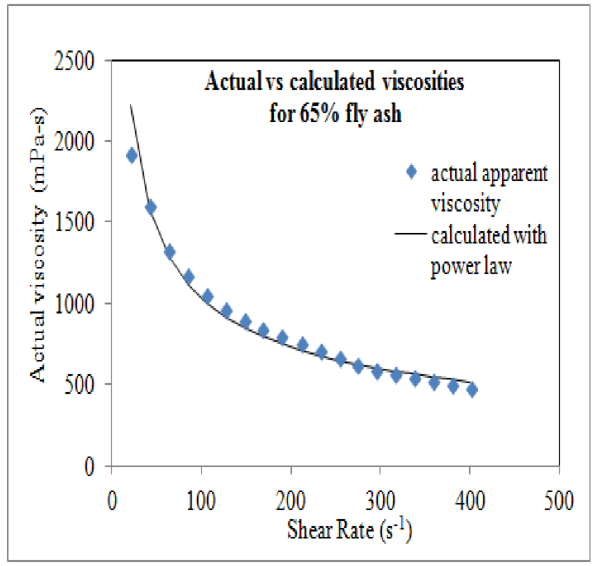

Figure 4.1.3f 60% fly ash slurry **Figure 4.1.3g 65% fly ash slurry**

It is observed from table 4.1.3c that value of viscosity index 'n' has value less than 1 for 40%, 50%, 60% and 65% which signifies that flow shows pseudoplastic behavior.

Every model has a certain minimum 'x' value below which it cannot predict accurate values. Above figures (4.1.3d to 4.1.3g) show that the accuracy of modeling by comparing it with actual viscosity values. It is observed that values at very low shear rates (less than $100s^{-1}$) are quite unpredictable using this model. The model works very well for higher shear rate (greater than $100s^{-1}$). It can be observed from figures 4.1.3f and 4.1.3g that the model worked very well for the wide range of shear rate (0 to $400s^{-1}$) at 60% and 65% concentrations. From figure 4.1.3f we can observe that at high concentration (60%) the 'x_{min}' of the model has decreased and is not predicting the viscosity value less than 150 s^{-1} shear rate. It can be concluded that no matter, how the concentration of fly ash is varied the model is highly capable of predicting accurate viscosity values greater than $120s^{-1}$, and at high shear rates it works better. The accuracy of model highly depends on the method of selection of data points used for regression. A careless selection process can be adversely deviate the calculated values from actual viscosity values. The modeling data is listed in Annexure A

Finally, from the rheological behavior of fly ash slurry it can be concluded that the rise in viscosity makes the use of higher concentrations difficult, even after the effect of additive on the drag reduction will not be better. At leaner mixture since drag reduction is low, so effect of additive is more as comparison to higher concentrations. On the other hand, 40%, 50% and 60% concentration lies in the middle and additives can reduce properties to an appreciable range. It would be predictable to experiment with these concentrations of fly ash slurry and see the effect of additives on it. Also from modeling analysis we can check that at 40%, 50% and 60% concentration of fly ash, the model worked well at which shear rates better. This shows that on the above thoughts, experiments are done with 40%, 50% and 60% fly ash concentration slurry. The results are discussed below.

4.2 Effect of additive on drag reduction at different concentration of fly ash slurry

4.2.1 Effect of detergent Ariel

In this section the effect of three different concentrations (1.5%, 1% and 0.5% by weight) of detergent Ariel at 40%, 50% and 60% is studied. Figure 4.2.1a to 4.2.1e compare the viscosity and shear rate values of slurry with and without detergent Ariel. It can be observed that from these figures that appreciable amount of reduction in viscosity is obtained in the shear rate range of 0 to $211s^{-1}$. Also in this range the effect produced by the 3 different dosages of additives is almost same. It can be observed that at higher shear rates (211 to $400s^{-1}$) there is a change in the pattern of viscosity curve, and we can observe from these figures that there is increase in viscosity in this range. If we observe closely, the change is not sudden and starts building up at $105s^{-1}$ and finally ready to flourish at $211s^{-1}$. Also we observe at 40% concentration this model give the accurate reading at shear rate of $295s^{-1}$, for 50% concentration this model give the accurate reading at shear rate of $232s^{-1.}$and for 60% concentration this model give more accurate reading at shear rate of $316s^{-1}$. Dosage of 1% additive is less effective as compare to other two concentrations of additive for 40% and 60% concentration.

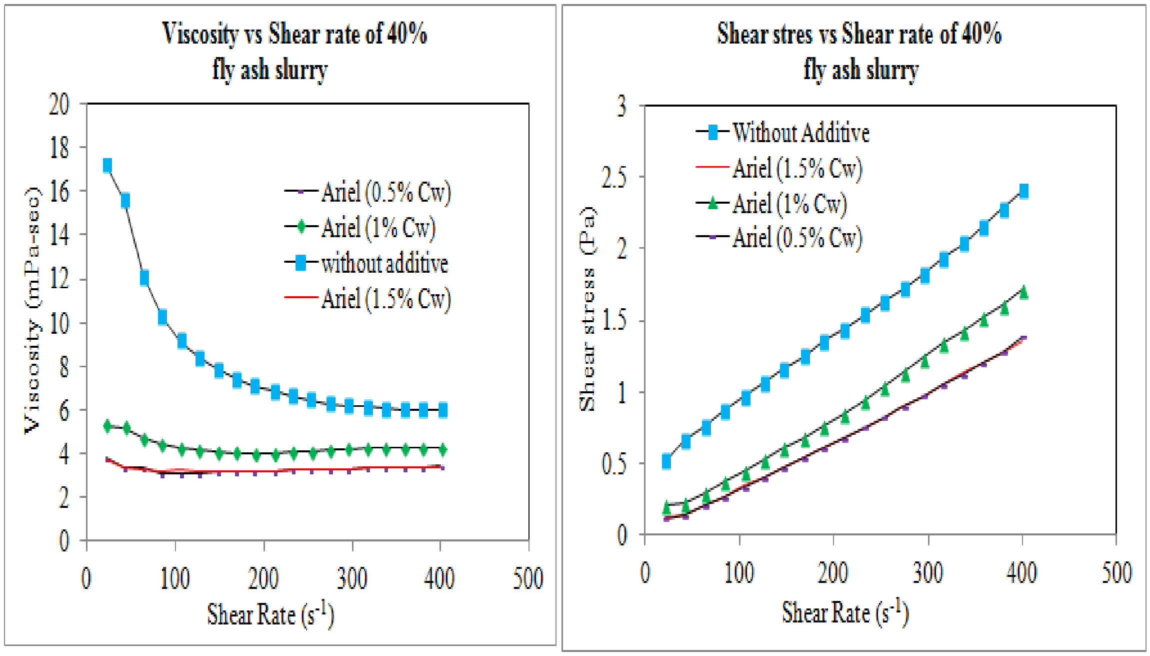

Figure 4.2.1 (a) Viscosity reduction with addition of detergent Ariel (b) Shear stress plot of slurry with and without detergent Ariel with 40% (by weight) fly ash concentration

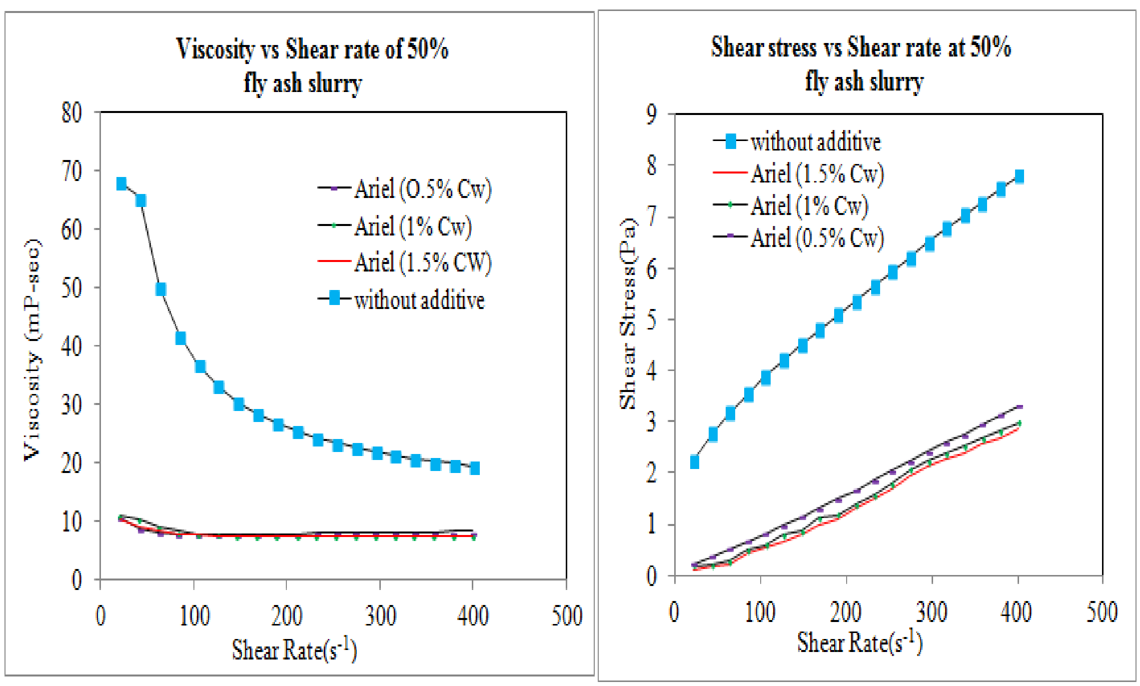

Figure 4.2.1 (c) Viscosity reduction with addition of detergent Ariel (d) Shear stress plot of slurry with and without detergent Ariel with 50% (by weight) fly ash concentration

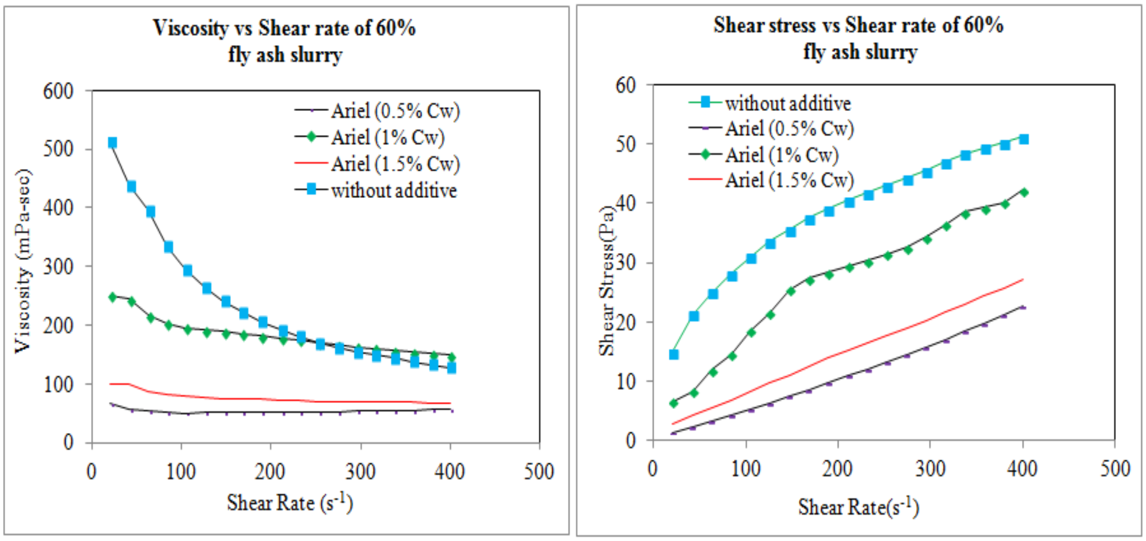

Figure 4.2.1 (e) Viscosity reduction with addition of detergent Ariel (f) Shear stress plot of slurry with and without detergent Ariel with 60% (by weight) fly ash slurry

4.2.2 Modeling of slurries containing detergent Ariel

In order to analyse the flow behavior of fly ash slurries (pseudoplastic or dilatant) modeling is necessary. The applicability of the model is estimating by observing the log-log plot as shown in figure 4.2.2a. Data points on log-log plot following a straight line patterns conforms the reliability of the model. Figure 4.2.2b shows the regression lines of data points drawn up to one standard deviation.

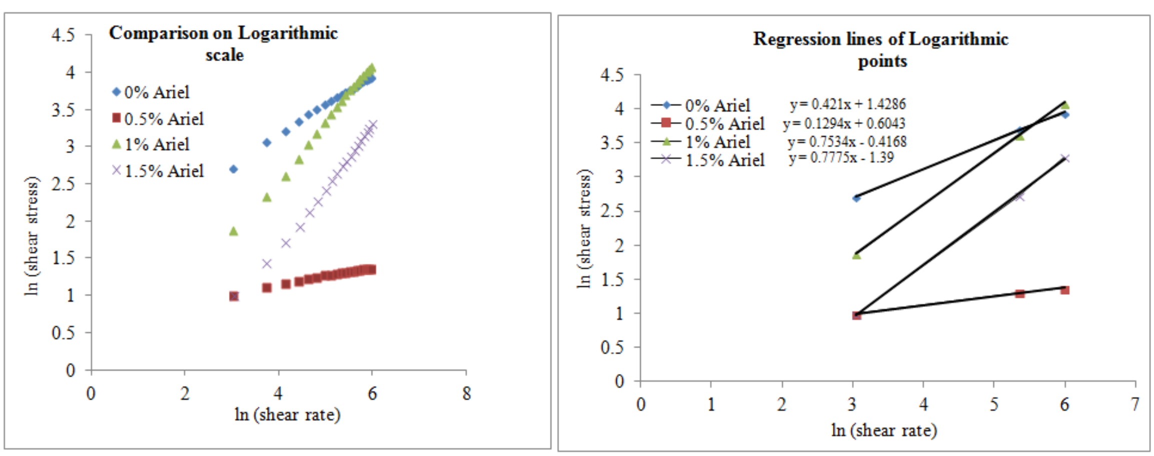

Figure 4.2.2 (a) Data points on log-log plot (b) Regression lines of points with equations on display

Coefficient of Correlation r			
r_1 (0% Ariel)	r_2 (0.5% Ariel)	r_3 (1% Ariel)	r_4 (1.5%Ariel)
0.9963	0.9865	0.9981	0.9955

Table 4.2.2c Coefficient of correlation 'r' of regression lines

slope = viscosity index (n)			
0% Ariel	0.5% Ariel	1% Ariel	1.5% Ariel
slope= 0.421	slope= 0.129	slope= 0.753	slope= 0.775
ln (K)= 1.4286 K= 4.172	ln (K)= 0.6043 K= 1.8299	ln (K)= -0.4168 K= 0.659	ln (K)= -1.39 K= 0.249

Table 4.2.2d Modeling parameters of slurries

Figures 4.2.2e to 4.2.2f compare the actual apparent viscosity values with modeled values. The results shows that at higher rates the viscosity obtained by power's law and apparent viscosity is same but at 0.5% of dosage it is different at all shear rates after calculated by Power's law for 60% fly ash slurry. It can be observed from table 4.2.2d that viscosity index 'n' increases with increase in the dosage of detergent Ariel conforming an increase in Shear-thinning behavior of slurry to increase in additive.

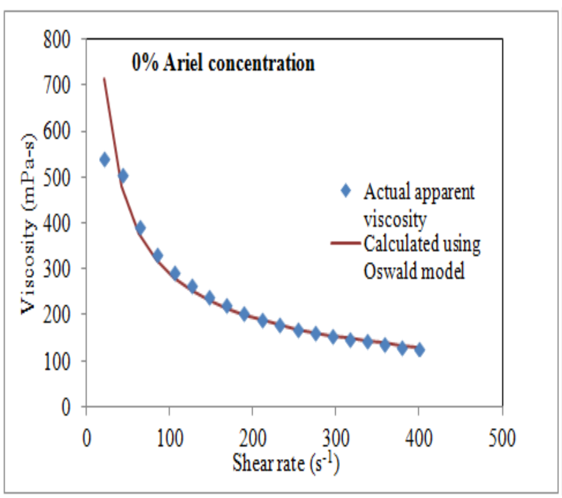

Figure 4.2.2e 60% fly ash slurry

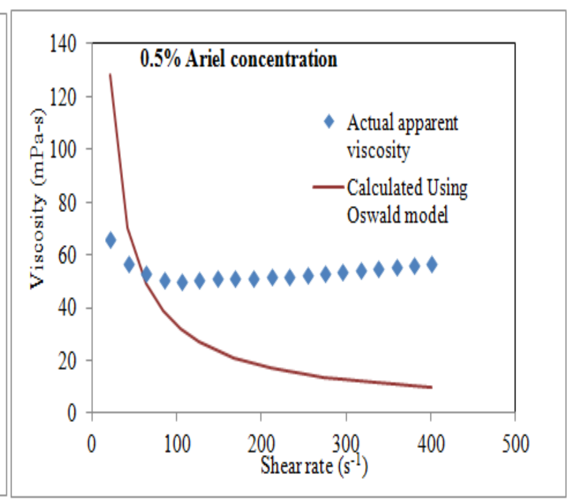

Figure 4.2.2f 60% fly ash slurry

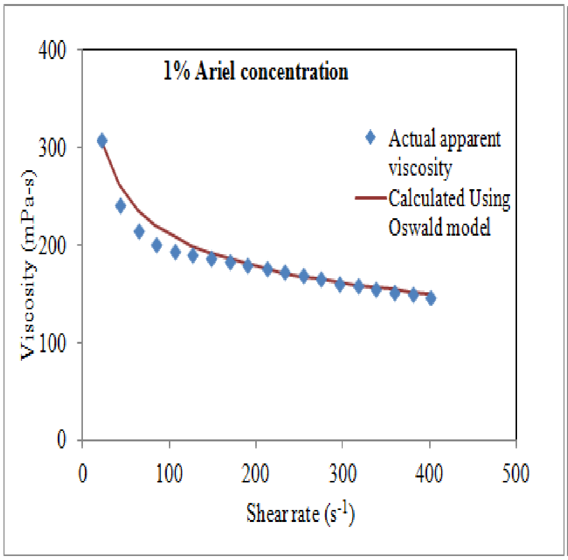

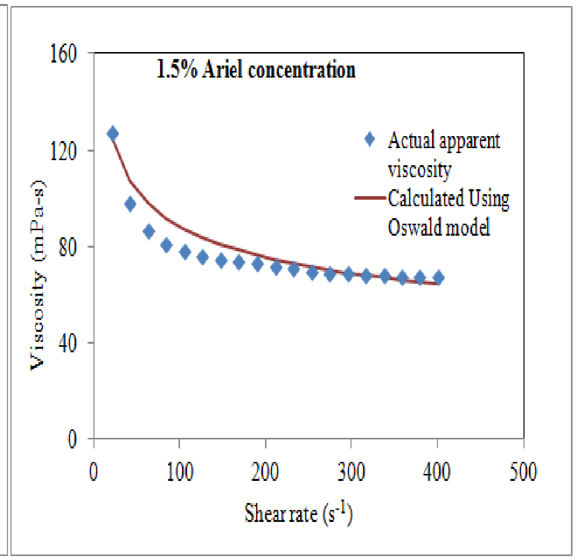

Figure 4.2.2g 60% fly ash slurry

Figure 4.2.2h 60% fly ash slurry

4.2.3 Effect of Glycerol on drag reduction

Glycerol is non-anionic in nature with a long hydrophobic tail. Figures 4.2.3a and 4.2.3b display the effect of different dosages of glycerol on Viscosity and shear stresses. It is observed that viscosity of slurry at 1% dosage of additive is less effective as comparison to dosage of 0.5% and 1% dosages of additive at 50% and 60%. The same phenomenon of aggregation of micelles at higher shear rates (more than 260s^{-1}) is observed. Results obtained from 1.5% and 0.5% of glycerol are better as compared 1% of glycerol at 50% concentration. But at 40% concentration of slurry the effect of additive at all dosage is same but result is that viscosity at all shear rates is becomes low after adding the additives. At this dosage the viscosity of slurry has reduced appreciably at low as well as high shear rates.

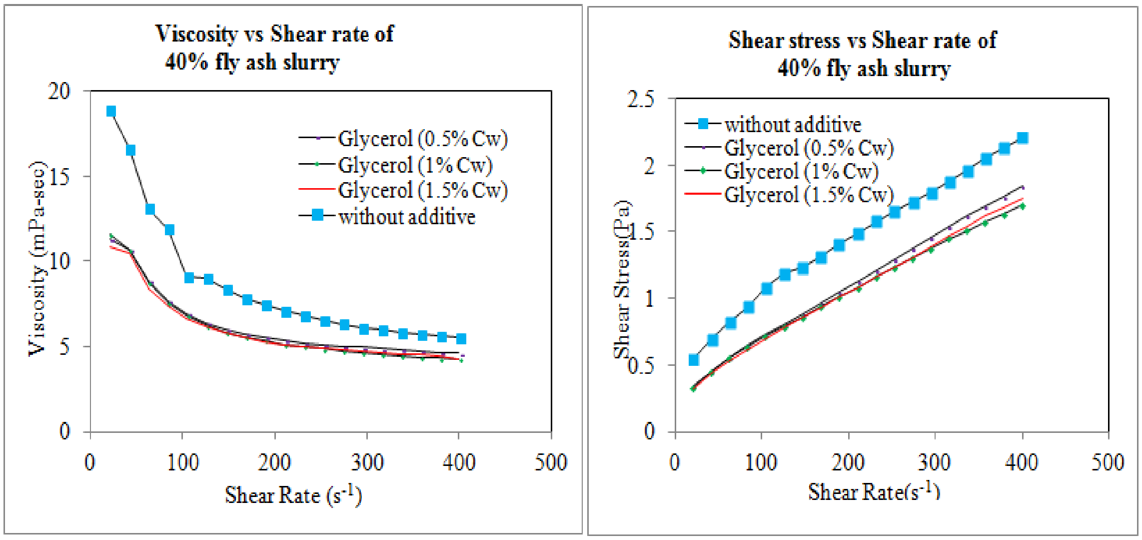

4.2.3 (a) Viscosity change with Glycerol (b) change in shear stresses of slurry using Glycerol with 40% (by weight) fly ash concentration

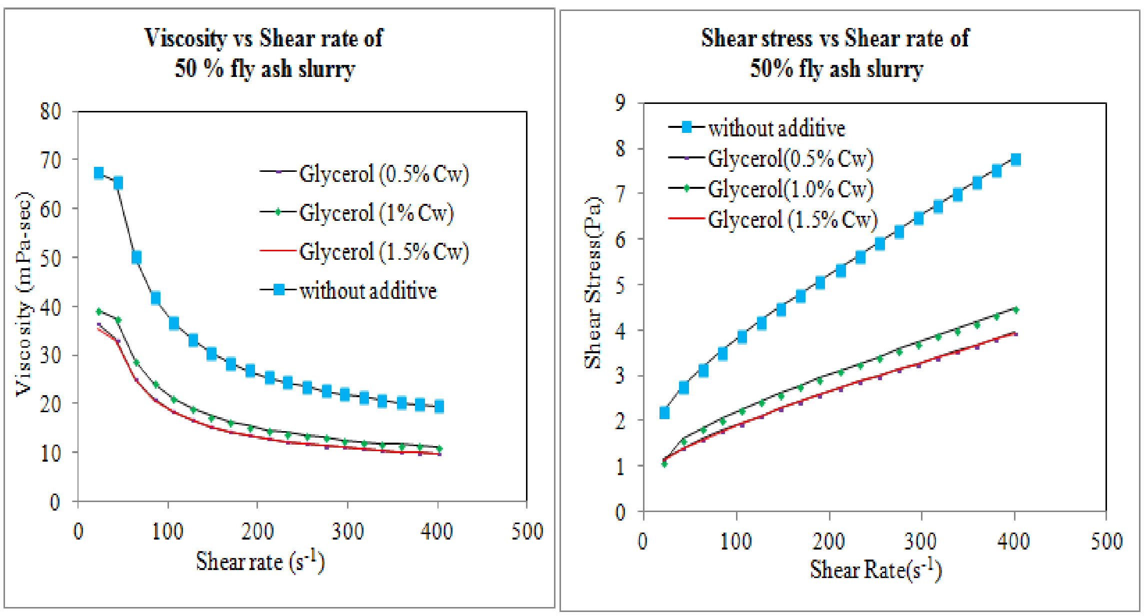

4.2.3 (c) Viscosity change with Glycerol (d) change in shear stresses of slurry using Glycerol with 50% (by weight) fly ash concentration

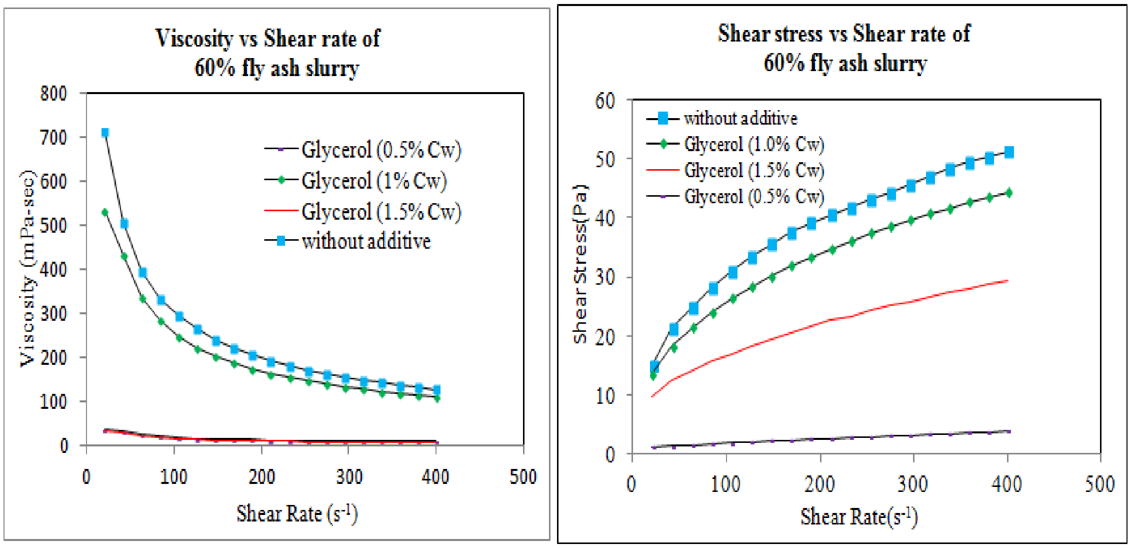

4.2.3 (e) Viscosity change with Glycerol (f) change in shear stresses of slurry using Glycerol with 60% (by weight) fly ash concentration

It is observed that for 60% fly ash slurry the optimal dosage of glycerol is 0.5% for which the viscosity is decreases as comparison to 1% and 1.5% additive as shown in Figure 4.2.3e and 4.2.3f.

4.2.4 Modeling of slurries containing Glycerol

It is observed that from log-log plot of shear and shear strain in figure 4.2.4a that the points approximate a straight line. Regression lines are plotted as in figure 4.2.4b. it is observed that value of n is less than 1for all dosage of additive, this shows that behavior remain pseudoplastic after adding the additive in the slurry. Linear line as a regression line on plot give the of value of slope ‘n’ and viscosity index ‘K’, with help of these values we can find out the value of the calculated viscosity at all shear rate with the help of power’s law.

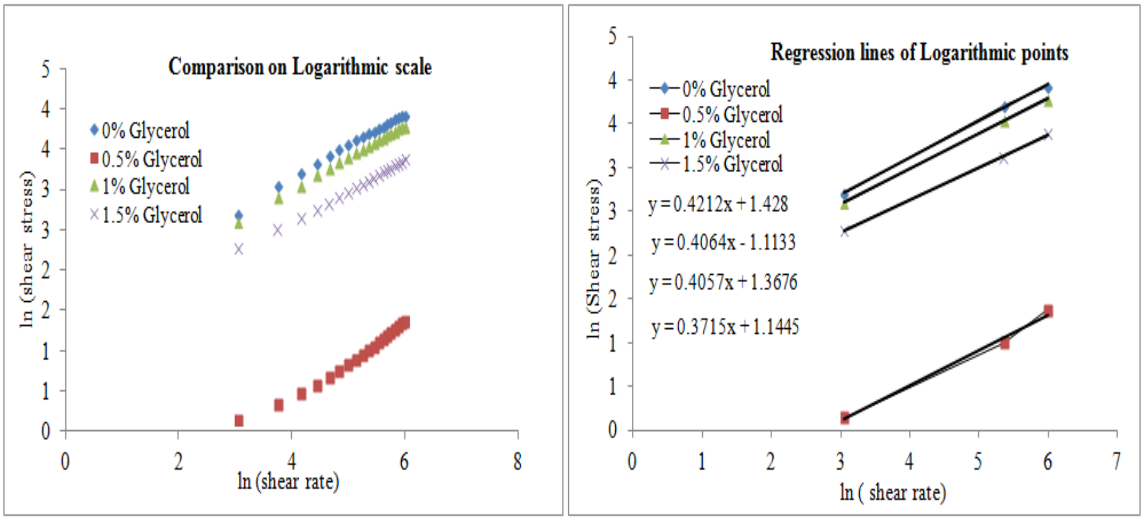

Figure 4.2.4 (a) Shear stress on logarithmic plot (b) Regression lines with equations on display

Coefficient of Correlation r			
r_1 (0% Glycerol)	r_2 (0.5% Glycerol)	r_3 (1% Glycerol)	r_4 (1.5% Glycerol)
0.9963	0.9822	0.9996	0.9978

Table 4.2.4c Coefficient of correlation 'r' showing the strength of regression

slope = viscosity index (n)			
0% Glycerol	0.5% Glycerol	1% Glycerol	1.5% Glycerol
slope= 0.4212	slope= 0.4064	slope= 0.4057	slope= 0.3715
ln (K)= 1.428	ln (K)= -1.1133	ln (K)= 1.3676	ln (K)= 1.445
K= 4.170	K= 0.328	K=3.926	K= 4.242

Table 4.2.4d Modeling parameters of slurries containing Glycerol

From the following figures (4.2.4e to 4.2.4h), we can observe that with increase in concentration of Glycerol in slurry, the modeled values start to deviate from actual values, it can be observed that at 1.5% glycerol the modeled values are not as approximately close to real viscosity values and even though viscosity is reduced flow behavior is not so smooth

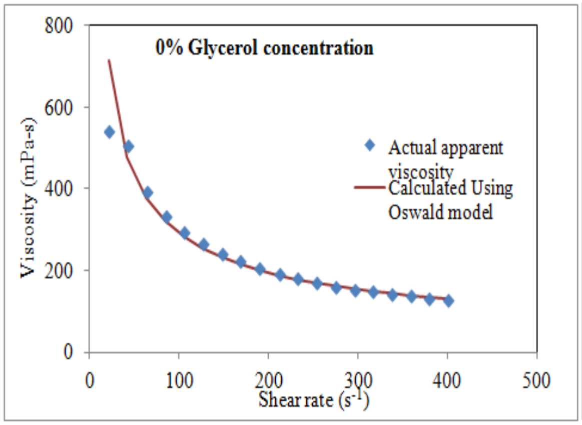

Figure 4.2.4e 60% fly ash slurry

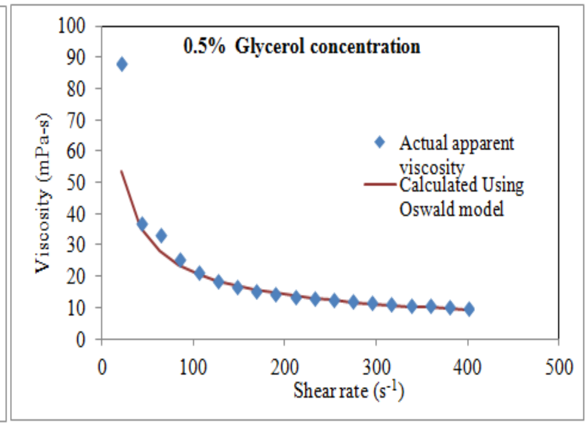

Figure 4.2.4f 60% fly ash slurry

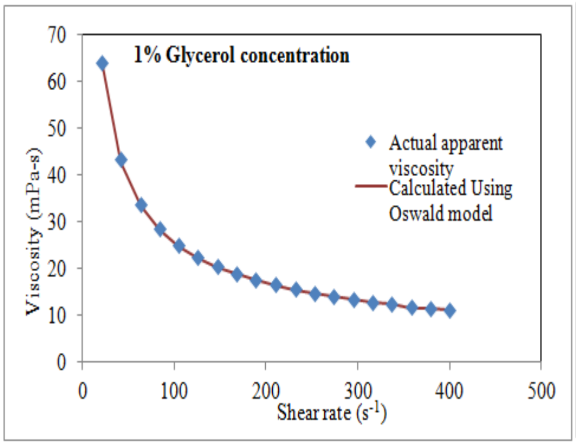

Figure 4.2.4g 60% fly ash slurry

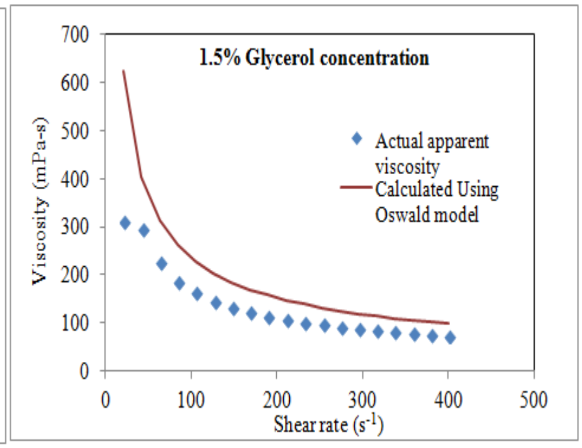

Figure 4.2.4h 60% fly ash slurry

4.2.5 Effect of polyethylene glycol on drag reduction

Polyethylene glycol is a non-ionic additive with hydrophobic hydrocarbon tail and polymer hydrophilic head with no charge. It is observed from Figure 4.2.5a and 4.2.5b that PEG effect on 40% slurry is not effective even though viscosity is increase from the apparent viscosity after adding the 1.5% concentration of PEG and also at higher shear rates viscosity is more at dosage of 0.5% and 1% PEG additive. This gives the result that at 40% fly ash concentration adding of PEG dosage is not effective as a reducing drag.

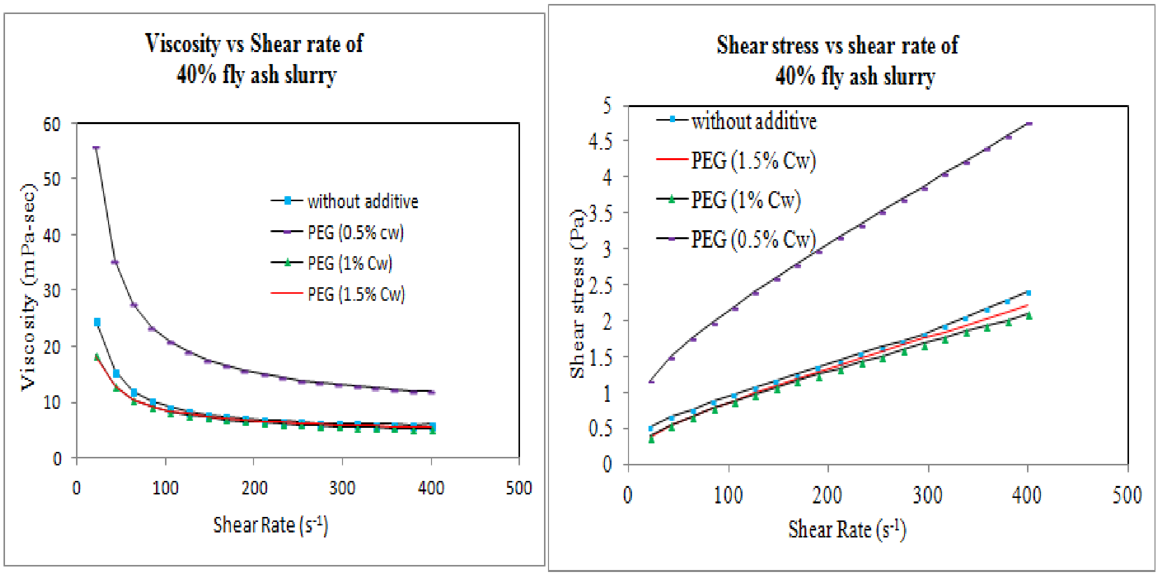

Figure 4.2.5 (a) Viscosity change with PEG (b) change in shear stresses of slurry using PEG with 40% (by weight) fly ash concentration

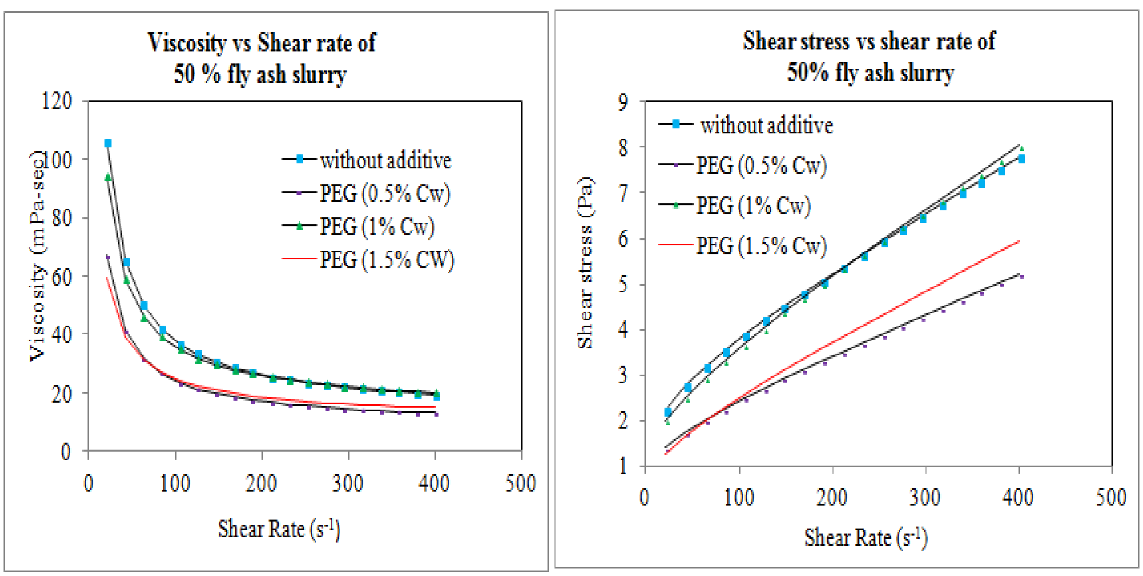

Figure 4.2.5 (c) Viscosity change with PEG (d) change in shear stresses of slurry using PEG with 50% (by weight) fly ash concentration

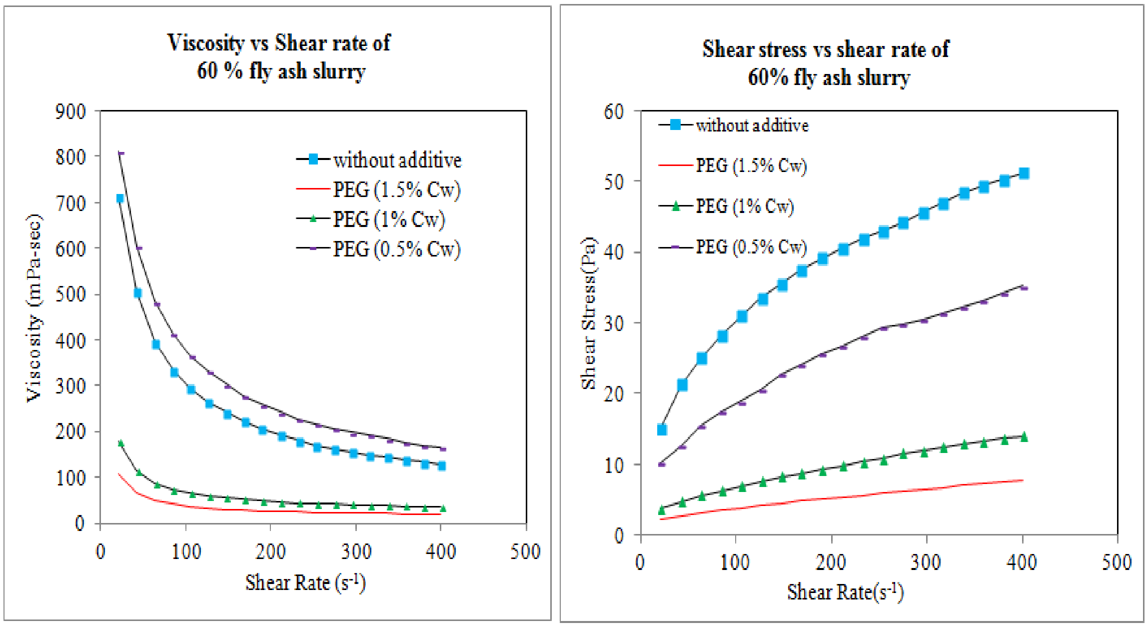

4.2.5 (e) Viscosity change with PEG (f) change in shear stresses of slurry using PEG with 60% (by weight) fly ash concentration

Figure 4.2.5c and 4.2.5d shows that dosage of additive at 50% fly ash concentration is no so effectives. From figure 4.2.5e and 4.2.5f it is clear that at 60% fly ash concentration dosage of 1.5% is more effective. Higher concentration of dosage of additive is more optimal at 60% concentration.

4.2.6 Modeling of slurries containing PEG

As previously stated, modeling of slurries containing PEG is a one way tool to conclude the reliability of the theory of reduction in wall friction. Figure 4.2.6a shows the data points of shear stress and shear strain on logarithmic plot.

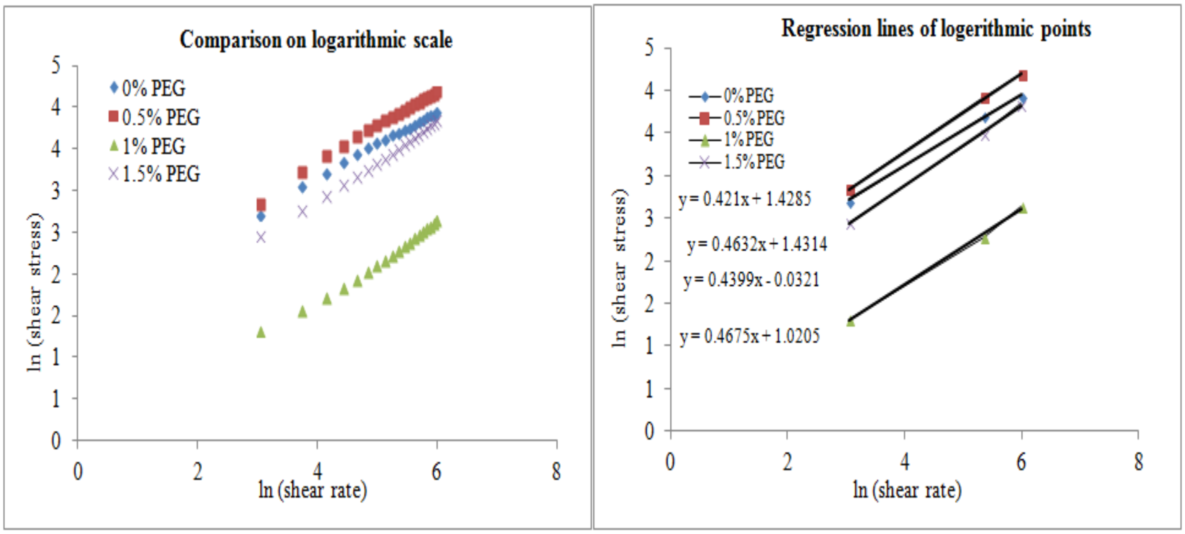

Figure 4.2.6 (a) log-log plot of shear stresses (b) Regression lines of logarithmic plot

Coefficient of Correlation r			
r_1 (0% PEG)	r_2 (0.5% PEG)	r_3 (1% PEG)	r_4 (1.5% PEG)
0.9963	0.9946	0.9911	0.9984

Table 4.2.6 Coefficient of regression ‘r’ of data points

Slope =viscosity index (n)			
0% PEG	0.5 % PEG	1% PEG	1.5% PEG
slope= 0.421	slope= 0.4632	slope= 0.4399	slope= 0.4675
ln (K)= 1.4285	ln (K)= 1.4314	ln (K)= -0.0321	ln (K)= 1.0205
K= 4.172	K= 4.184	K= 0.968	K=2.774

Table 4.2.6d Modeling parameters for slurries containing PEG

Results of modeling are shown below, which indicates smooth flow behavior of slurry. From figure 4.2.6g, apparent viscosity values of slurry containing PEG lies very close to modeled values even at low shear rates such as $42.1s^{-1}$. Modeling data is listed in Annexure B

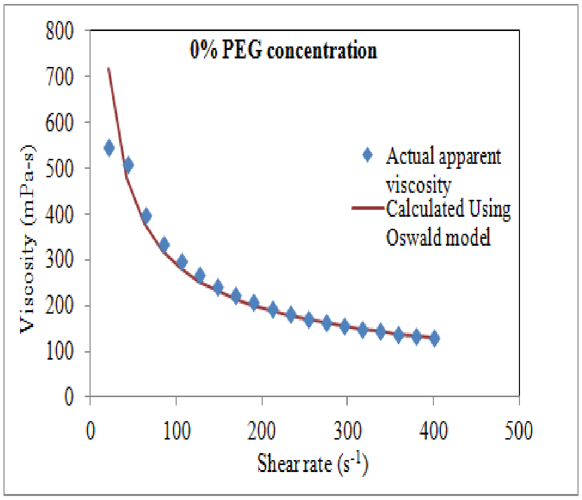

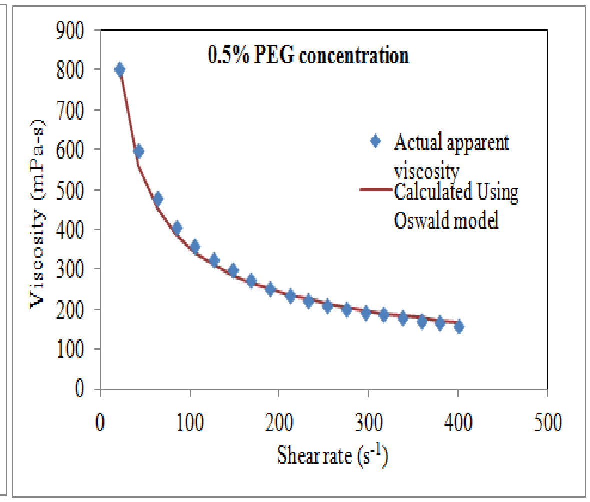

Figure 4.2.6e 60% fly ash slurry **Figure 4.2.6f 60% fly ash slurry**

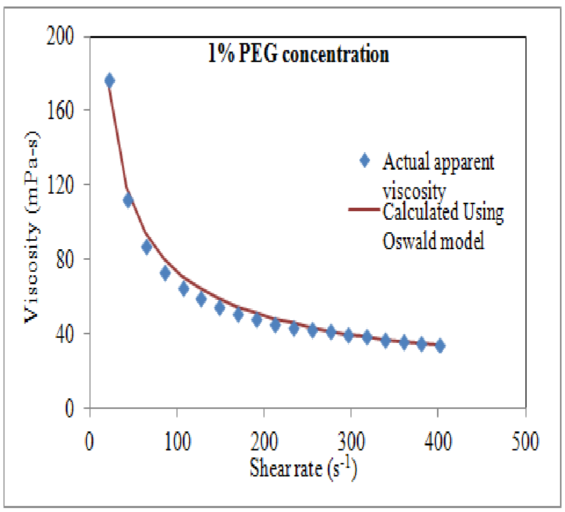

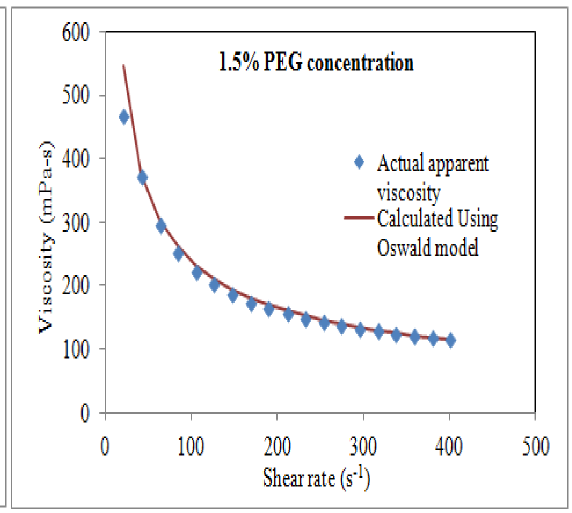

Figure 4.2.6g 60% fly ash slurry **Figure 4.2.6h 60% fly ash slurry**

4.2.7 Effect of SLS on drag reduction

SLS is anionic in nature with a long hydrophobic tail. Figure 4.2.7a to 4.2.7f display effect of different dosages of SLS on viscosity and shear stresses at 40%, 50% and 60% concentration (by weight) fly ash slurry. It is observed that viscosity of slurry decreases with increases in dosage of SLS. The same phenomenon of aggregation of micelles at higher shear rates (more than 274s^{-1}) is observed. Results obtained from 1.5% of SLS are better as compared to 0.5% and 1% SLS. At this dosage the viscosity of slurry has reduced appreciably at low as well as high shear rates. The use of high dosage of SLS is also economical, as it is derived from inexpensive soap and shampoo and hence has its cheap manufacturing cost.

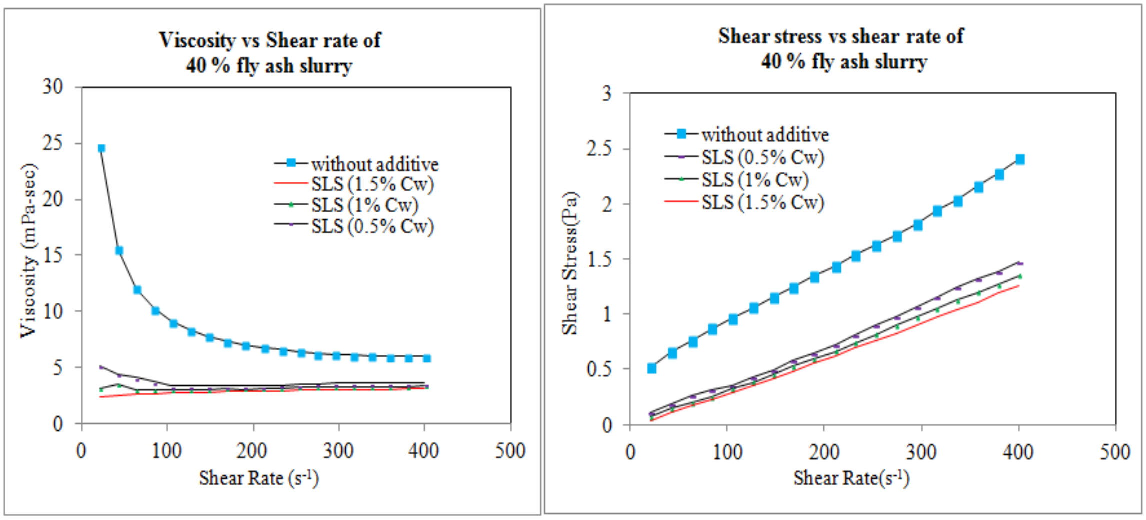

Figure 4.2.7 (a) Effect of SLS on viscosity (b) Reduction in shear stress of slurry using SLS with 40% (by weight) fly ash concentration

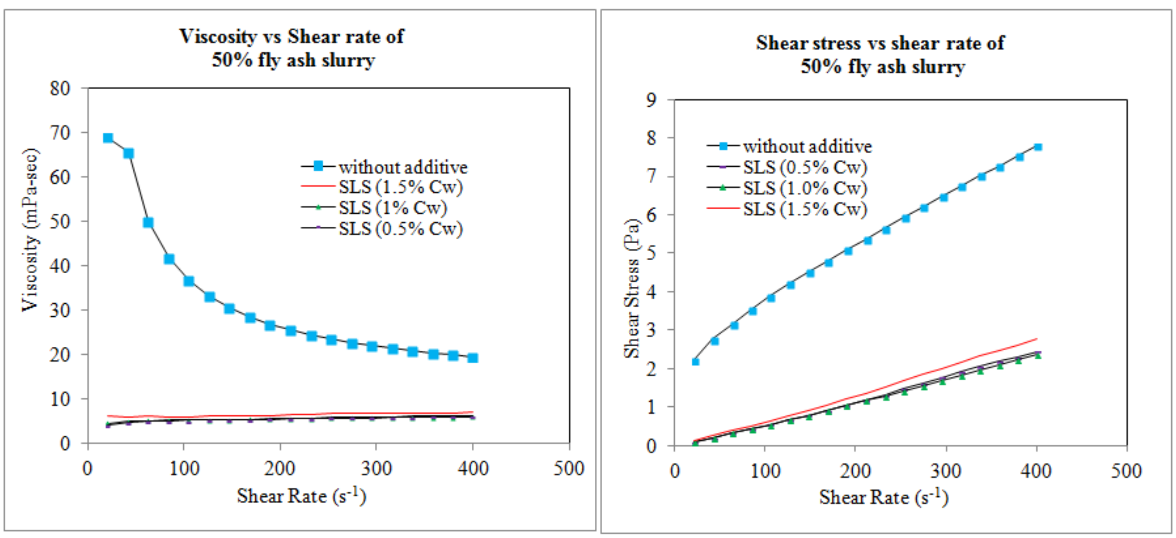

Figure 4.2.7 (c) Effect of SLS on viscosity (d) Reduction in shear stress of slurry using SLS with 50% (by weight) fly ash concentration

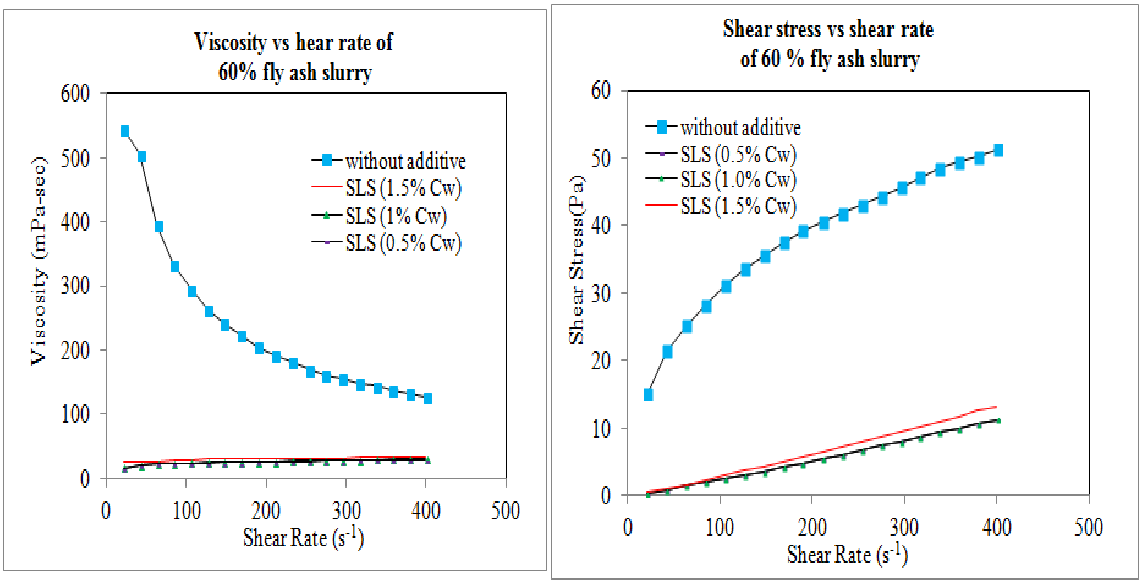

Figure 4.2.7 (e) Effect of SLS on viscosity (f) Reduction in shear stress of slurry using SLS with 60% (by weight) fly ash concentration

From figure 4.2.7c and 4.2.7d it is observed that 1% dosage of SLS is more optimal as comparison dosages of 0.5% and 1.5% of SLS and also observed from the figure 4.2.7e and 4.2.7f that SLS additives works better at higher concentration (60% fly ash slurry). Even 0.5% dosage of SLS creates more effect to reduce the viscosity to large extent. Dosages of SLS as compares to others additives are more optimal to help the drag reduction at higher concentration also. From figure 4.2.7e and 4.2.7f it is cleared that at higher concentration also dosages is more optimal (0.5%, 1% and 1.5%).

4.2.8 Modeling of slurries containing SLS

It is observed from log-log plot of shear stress and shear strain in figure 4.2.8a that approximate a straight line. Regression lines are plotted as in figure 4.2.8b

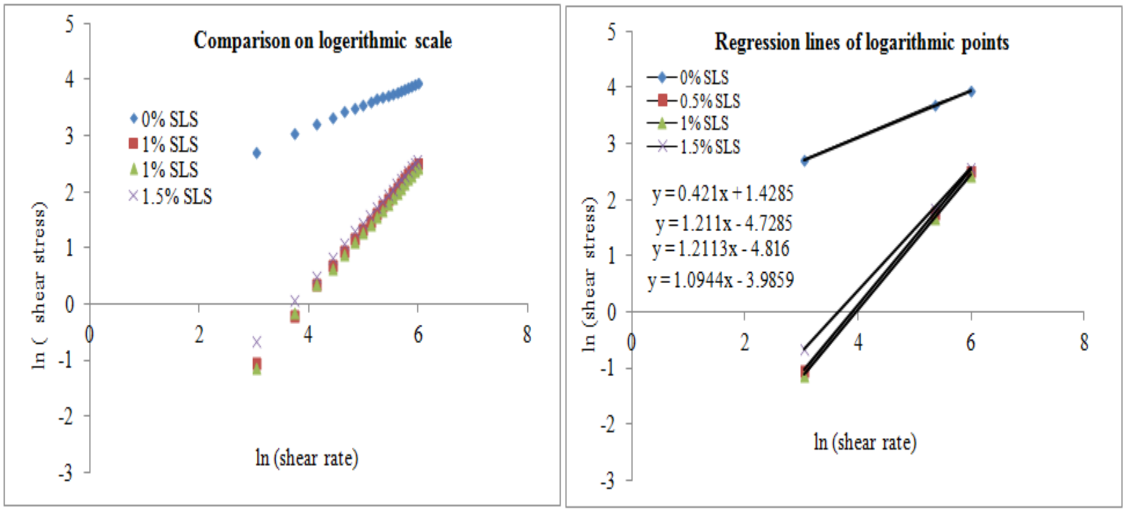

Figure 4.2.8 (a) log-log plot of shear stress (b) Regression lines of logarithmic plot

Coefficient of Correlation r			
r_1 (0% SLS)	r_2 (0.5% SLS)	r_3 (1% SLS)	r_4 (1.5% SLS)
0.9963	0.9994	0.9984	0.9997

Table 4.2.8c Coefficient of regression 'r' of data points

slope=viscosity index (n)			
0% SLS	0.5% SLS	1% SLS	1.5% SLS
slope= 0.421	slope= 1.211	slope= 1.2113	slope= 1.0944
ln (K)= 1.4285 K= 4.172	ln (K)= -4.7285 K= 0.00088	ln (K)= -4.816 K= 0.000809	ln (K)= -3.9859 K= 0.01857

Table 4.2.8d Modeling parameters for slurries containing SLS

Results of modeling are shown below, which indicates smooth flow behavior of slurry. From figure 4.2.8f, apparent viscosity values of slurry containing SLS lies very close to modeled values even at low shear rates such as 62.1s^{-1}. Modeled data is listed in Annexure B

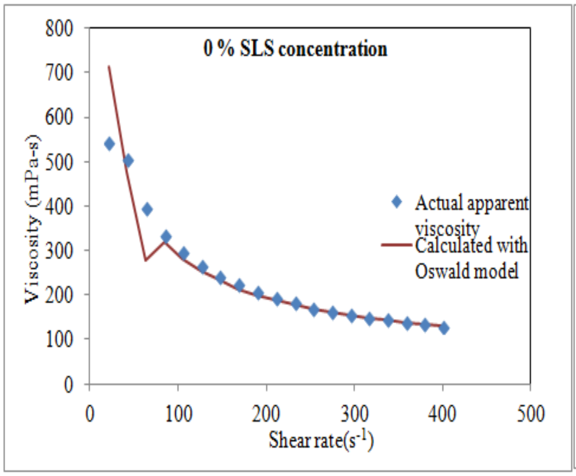

Figure 4.2.8c 60% fly ash slurry

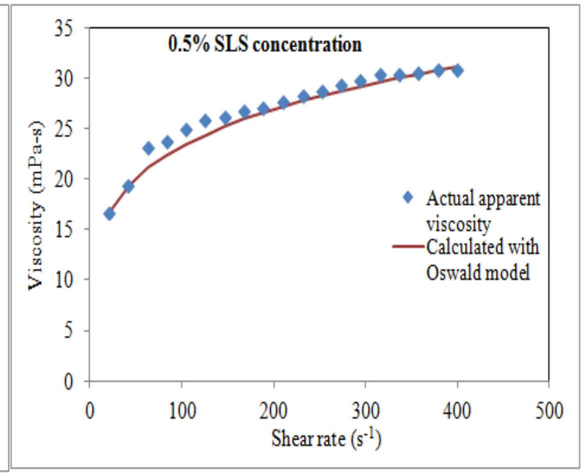

Figure 4.2.8d 60% fly ash slurry

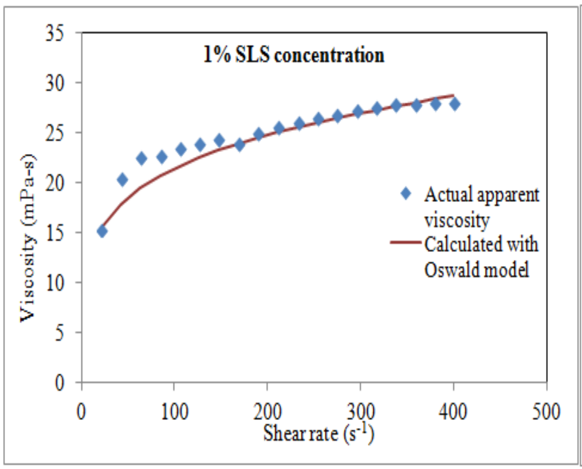

Figure 4.28e 60% fly ash slurry

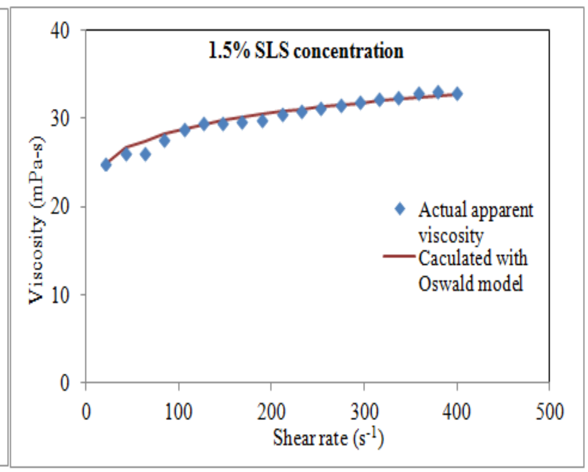

Figure 4.2.8f 60% fly ash slurry

The data involved is listed in Annexure B

4.3 Comparison between the Drag reduction capabilities of Detergent Ariel, Glycerol, PEG and SLS

From 4.3a and 4.3.b it is observed that the additive polyethylene glycol is not so effective for drag reduction at 40% fly ash slurry. The effect of SLS and detergent Ariel is more effective. From figure 4.3c and 4.3d it is cleared that 1% additive concentration show the same results as that of 0.5% additive concentration but in both these concentrations SLS and detergent Ariel give the most effective drag reduction all shear rates (0 to 400s^{-1}).

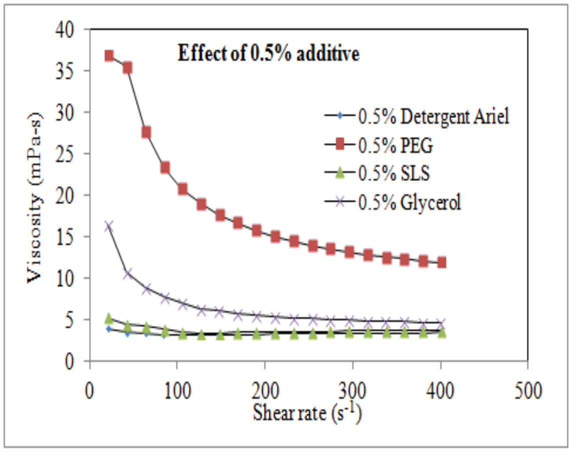

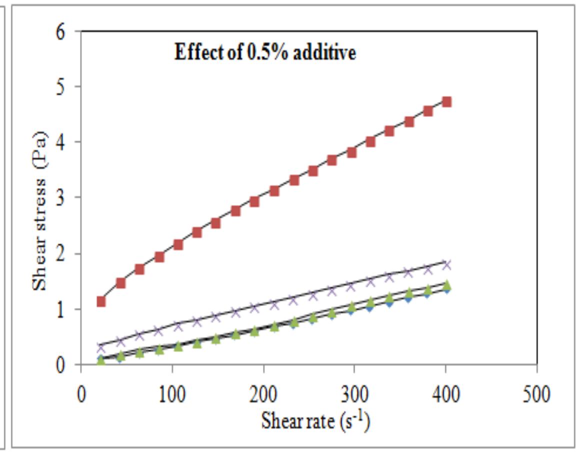

Figure 4.3a 40% fly slurry

Figure 4.3b 40% fly ash slurry

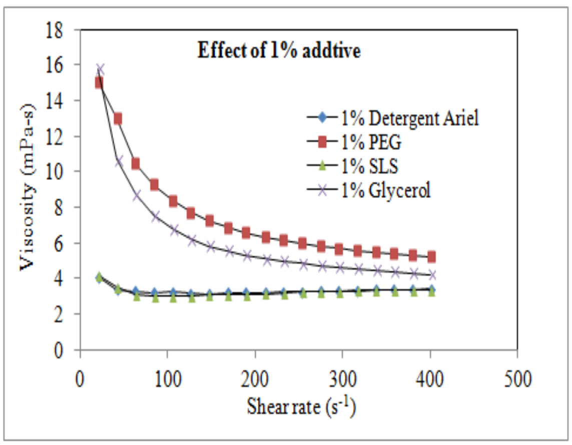

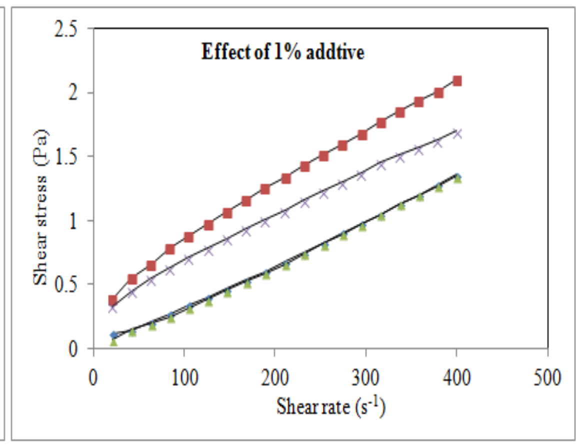

Figure 4.3 c 40% fly ash slurry

Figure 4.3d 40% fly ash slurry

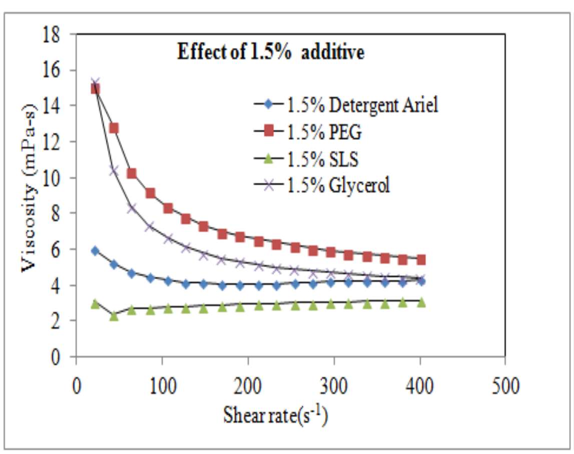

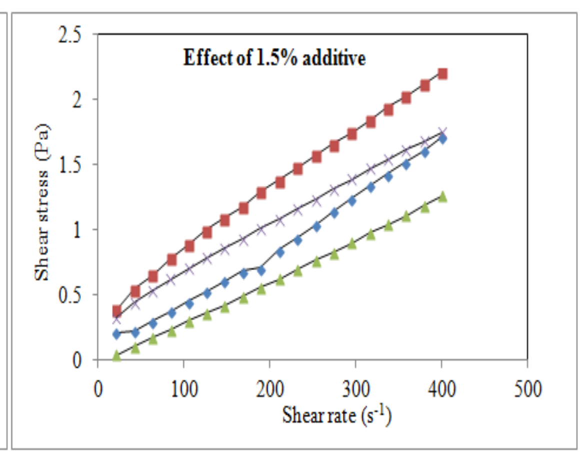

Figure 4.3e 40% fly ash slurry

Figure 4.3f 40% fly ash slurry

From figure 4.3e and 4.3f it is observed that SLS is more effective as comparison to others three additives. Glycerol and PEG is not so effective as comparison to detergent Ariel and SLS.

CHAPTER 5

CONCLUSION AND RECOMMENDATIONS

5.1 Conclusions

1. The study of flow behavior of slurry at different concentrations of fly ash indicates that viscosity increase with increase in concentration.
2. At higher concentration (40%, 50%, 60% and 65%) behavior of slurry is pseudoplastic or shear-thinning. It is observed that at higher concentrations modeling is necessary in order to predict the flow behavior of slurry.
3. A comparative study between the effects created by the additives shows that PEG is less effective in reducing viscosity, but more effect is created by SLS, after that detergent Ariel and then Glycerol.
4. Dosage of 1% detergent Ariel is less effective as compare to concentrations (0.5% and 1.5%) of additive for 40% and 60% fly ash slurries.
5. At 65% concentration viscosity at shear rate $274s^{-1}$ is 625mPa-s which is very high as comparison to other concentration (40%, 50% and 60%) indicates that high concentration of fly ash disposal remains very difficult with additive.
6. Viscosity of slurry at higher concentration reduces by the addition of SLS, viscosity decreases with increase in dosage of SLS. Best dosage of SLS is 1.5% at which viscosity is minimum both at low and high shear rates.
7. Even small dosage of Glycerol (such as 0.5% Cw), viscosity of slurry at 60% fly ash slurry reduced drastically, also consistency coefficient ‘K’ decreases with each increase in Glycerol dosage. Optimal dosage is observed to be 0.5%, in which aggregation of micelles is minimum and decrease in viscosity is miximum both at low and high shear rates.
8. Flow behavior of slurries containing detergent Ariel is improved, and is confirmed by the modeling results, in which the calculated value of viscosities with Power’s law lie very close to actual apparent viscosities at all shear rates.

9. Power's law model give the best result at higher rates above $211 s^{-1}$ and at low shear rates calculated viscosities is don't match the equal to actual apparent viscosities at higher concentrations.

Recommendations for future work

Some recommendations for future work are as follows

1. The study involved in this work deals with the mainly the effect on viscosity of slurry at higher concentrations with the help of Power's law model, however flow behavior is not fully defined by just viscosity. It also deals with surface tension, temperature and turbidity of the flow, due to time limitation a detail study on these parameters is not carried out, it is recommended to work on these parameters and flourish the study of flow behavior of slurry to its full extent.
2. After studying the properties of fly ash check out the leaching effect on agriculture land and what effects on disposal area of the fly ash near power plant.
3. Based on time limitations a simple rheological model (Power's law model) is used to predict the flow behavior, but recommended that compare the results with others rheological models (Bingham's model and Harschel-Bulkley model) to check the existent model for above 65% fly ash slurries.
4. In this work the study of SLS ON 40%, 50% and 60% fly ash slurries is carried out without the use of counterion. Anionic surfactants like SLS give better results when used in conjuction with counter ion sodium salycylate, due to time limitation a study on counter ions is carried out. Now since the effect of SLS on high concentration slurries have been confirmed, it is an appropriate counter ion, to increase its effect of viscosity reduction and prevent micelle aggregation.

REFERENCES

1. Chandel S., Singh S.N., Seshadri V., (2010), deposition characteristics of coal ash slurries at higher concentrations, Advanced Powder Technology 20, 383-389.

2. B. Bournonville, A. Nzihou, (2002), rheology of non-newtonian suspensions of fly ash: effect of concentration, yield stress and hydrodynamic interactions, Powder Technology 128,148–158.

3. P.K. Senapati, B.K. Mishra, A. Parida, (2010), modeling of viscosity for power plant ash slurry at higher concentrations, effect of solids volume fraction, particle size and hydrodynamic interactions, Powder Technology 197, 1–8.

4. Kamal El-Nahhas, Nageh Gad El-Hak, Magdy Abou Rayan and Imam El-Sawaf, (2009), effect of particle size distribution on the hydraulic transport of settling slurries, Thirteenth International Water Technology Conference, IWTC13, Hurghada Egypt.

5. VR Kumar Vedapalli, Leslie Petrik, Veruscha Fester, Paul Slatter and Gervais, (2007), effect of Fly Ash particle size on its capacity to neutralize Acid Mine Drainage and influence on the rheological behavior of residual solids, World of Coal Ash (WOCA), Northern Kentucky, USA.

6. Naik H.K., Mishra M.K., Ro Karanam U.M., (2009), the effect of drag reducing additives on the rheological properties of fly ash-water Suspensions at varying temperature Environment, Coal Combustion and Gasification Products, 25-31,doi:10.4177/CCGP-D-09-0005.1.

7. Carmel Jolicoeur, Thi Cong To, Thue Soan Nguyen, Russell Hill and Monique Page (2009), mode of anionic surfactant for air entrainment in cement Pastes w-w/0 Fly Ash, World of Coal Ash (WOCA) Conference, in Lexington, Ku, USA.

8. Elizabet M. Vano der Merwe, Linda Petrik, Veruscha Fester, Paul Slater and Gervais Sery (2007), effect of fly ash particle size of its capacity to neutralize acid mine drainage and influence on the rheological behavior of residual solids, World of Coal Ash (WOCA), Northern Kentucky, USA.

9. Shunsuke Hashimoto and Kazushi Kawamura (2012), viscosity reduction with Self-Assembly of Cationic Surfactant on Tetra-n-butyl Ammonium Bromide Semi-Clathrate Hydrate Aqueous Slurry, American Chemical Science Journal 2(3): 69-85.

10. Dr V Seshadri, Dr SN Singh, KK Jain, Dr AK Verma (2008), effect of additive on Head Loss in the high concentration slurry disposal of fly ash.

11. Chandel, Sunil , Seshadri, V. and Singh, S. N.(2009), Effect of Additive on Pressure Drop and Rheological Characteristics of Fly Ash Slurry at High Concentration, Particulate Science and Technology, 27: 3, 271-284.

12. http:// en.wikipedia.org/wiki/Fly ash-Fly classification and utilization

13. Dhir, R.K. (2005), emerging, trends in fly ash utilization: world scenario, Proc. Of International Conference on fly ash utilization, pp: 0 1.1-1.10.

14. Slurry pipe line transportation by E.J. Wasp, series of bulk material handling, Vol.1, Tranc Tech Publication, 1977.

15. Pankaj Dewangan, Dr. Manoj Pradhan, Dr. Naval Kishore, Utilization of fly ash as structural fill material for safe and sustainable development, need of the hour, the Indian mining an engineering journal, MineTECH'10.

16. Lei Li, Hiromoto Usui & Hiroshi Suzuki (2002), study of Pipeline Transportation of Dense Fly Ash-Water Slurry, Coal Preparation, 22:2, 65-80.

17. S. K. Mishra, P. K. Senapati & D. Panda (2002), rheological behavior of Coal-Water Slurry, Energy Source, 24:159-167.

18. Dule P. Bentz, Chiara F. Ferraris (2010), rheology and setting of high volume fly ash mixtures, Cement & Concrete Composites 32,265-270.

19. Rajan Bhattacharjee, Animul Laskar (2010), Rheological behavior of Fly Ash based geopolymer Concrete, 35th Conference on our world in concrete & structures, Singapore.

20. Hrushi K. Naik, Manoj K. Mishra, and Karanam U. M. Rao (2011), evaluation of flow characteristics of fly ash slurry at 40% solid concentration with and without additive, world of coal ash (WOCA) conference-May 9-12, in Denver, USA.

21. H. K. Naik, M.K. Mishra, U. M. Rao Karanam, D. Deb (2009), evaluation of the role of a cationic surfactant on the flow characteristics of fly ash slurry, Elsevier B.V.

22. Ferhat Hadri, Anthony Besq, Sylvain Guillou, Rachid Makhloufi (2011), Temperature and concentration influence on drag reduction of very low concentrated CTAC/NaSal aqueous solution in turbulent pipe flow, J. Non-Newtonian Fluid Mech.166, 326-33.

23. Hiromoto Usui, Lei Li and Hiroshi Suzuki (2001), rheology and pipeline transportation of dense fly ash-water slurry, Korea-Australia Rheology Journal, Vol. 13, No. 1, pp. 47-54.

24. Monoj Sharma, Chandan Guria, Ashis Sarkar and Akhilendra K. Pathak (2012), recycle of waste fly ash, International Journal of Science, Environment and Technology, Vol. 1, No 4, 2012, 285 – 301.

25. K.B Anoop, S.Kabelec, T. Sundarajan and Sarit K. Das (2009), rheological and flow characteristics of nanofluids, Influence of electroviscous effects and particle agglomeration. J. Appl. Phy.106, 034909.

26. Sunil Chandel, S. N. Singh and V. Seshadri (2010), transportation of High Concentration Coal Ash Slurries through Pipelines, International Archieve of Applied science & Technology, Vol. 1, 1-9.

27. K. SIMON**,** the role of different rheological models in accuracy of pressure loss prediction, UDK 622.244.442:532.58.

28. Jiabin Fu, Challenges to increased use of coal combustion products in China, spring 2010, Linkopings Universitet.

29. Jean-Louis, Salager (2002), Laboratory of formulation interfaces rheology and process

30. Anton paar German manufactured user manual of rheometer, Rheolab QC Rotational rheometer for quality control.

31. Freedman D., Pisani R., Purves R., (2009), statistics, Viva Books private limited, ISBN -13: 978-81-309-1055.

32. L Chahine., N Sempson., C Wagoner., (1997), the effect of sodium lauryl sulfate on recurrent aphthous ulcers: a clinical study, Compend Contic Educ Dent 18, No. 12. 1238-40. PMID 9656847.

33. Final report on the safety assessment of sodium lauryl sulfate and ammonium lauryl sulfate, International journal of toxicology 2, No. 7, 127-181.

34. GEHO positive displacement slurry pumps high concentration slurry disposal solution.

35. Verma Abhai Kumar, S.N and Seshadri (2004), effect of particle size distribution on rheological properties of fly ash slurries at high concentrations, international journal of "Applied rheology", Zurich, Switzerland, Accepted for Publication.

ANNEXURE A

FLOW BEHAVIOUR OF SLURRY

40% Fly ash				
Meas. Pts.	Time(sec)	Viscosity (m Pa-sec)	Shear Rate (per sec)	Shear Stress (Pa)
1	6	#######	0.00009	0.00027
2	12	16.7	21.1	0.519
3	8	15.6	42.1	O.659
4	24	12.1	63.2	0.763
5	30	10.3	84.2	0.868
6	36	9.16	105	0.964
7	42	8.41	126	1.06
8	48	7.86	147	1.16
9	54	7.43	168	1.25
10	60	7.11	189	1.35
11	66	6.85	211	1.44
12	72	6.64	232	1.54
13	78	6.45	253	1.63
14	84	6.3	274	1.72
15	90	6.19	295	1.82
16	96	6.15	316	1.94
17	102	6.07	337	2.04
18	108	6.03	358	2.16
19	114	6.02	379	2.28
20	120	6.03	400	2.41

Table A.1 rheometer data for 40% fly ash

50% Fly ash				
Meas. Pts	Time (sec)	Viscosity (m Pa-sec)	Shear Rate (per sec)	Shear Stress (Pa)
1	6	#######	0.000111	0.0471
2	12	106	21.1	2.2
3	18	65.5	42.1	2.76
4	24	50.1	63.2	3.16
5	30	41.9	84.2	3.53
6	36	36.8	105	3.88
7	42	33.3	126	4.2
8	48	30.5	147	4.5
9	54	28.5	168	4.79
10	60	26.8	189	5.08
11	66	25.5	211	5.36
12	72	24.4	232	5.65
13	78	23.5	253	5.93
14	84	22.7	274	6.2
15	90	22	295	6.49
16	96	21.4	316	6.76
17	102	20.8	337	7.02
18	108	20.3	358	7.27
19	114	19.9	379	7.54
20	120	19.5	400	7.79

Table A.2 rheometer data for 50% fly ash slurry

60% Fly ash				
Meas. Pts	Time (sec)	Viscosity (m Pa-sec)	Shear Rate (per sec)	Shear stress (Pa)
1	6	#######	0.0005	0.0658
2	12	544	21.1	15
3	18	506	42.1	21.3
4	24	395	63.2	25
5	30	334	84.2	28.2
6	36	295	105	31
7	42	265	126	33.5
8	48	241	147	35.5
9	54	223	168	37.5
10	60	206	189	39.1
11	66	192	211	40.5
12	72	181	232	41.8
13	78	170	252	43
14	84	162	274	44.2
15	90	155	295	45.6
16	96	149	316	47
17	102	144	337	48.4
18	108	138	358	49.4
19	114	133	379	50.2
20	120	128	400	51.2

Table A.3 rheometer data for 60% fly ash slurry

65% Fly ash				
Meas. Pts	Time (sec)	Viscosity (m Pa-sec)	Shear Rate (per sec)	Shear Stress (Pa)
1	6	#######	0.000591	0.0658
2	12	1930	21.1	40.7
3	18	1600	42.1	67.3
4	24	1330	63.2	84.1
5	30	1170	84.2	98.6
6	36	1050	105	110
7	42	966	126	122
8	48	899	147	132
9	54	847	168	143
10	60	805	189	152
11	66	758	211	160
12	72	709	232	164
13	78	665	253	168
14	84	625	274	171
15	90	593	295	175
16	96	567	316	179
17	102	543	337	183
18	108	520	358	186
19	114	498	379	189
20	120	477	400	191

Table A.4 rheometer data for 65% fly ash slurry

40% fly ash					
Shear Rate (γ) [per sec]	Shear Stress (τ) [Pa]	ln (γ)	ln (τ)	Actual apparent viscosity (m Pa-sec)	Calculated viscosity
0.0009	0.00027	-7.0131	-8.21	#######	222.60
21.1	0.519	3.049	-0.655	16.7	20.85
42.1	0.659	3.74	-0.4170	15.6	15.14
63.2	0.763	4.146	-0.270	12.1	12.53
84.2	0.868	4.43	-0.141	10.3	10.3
105	0.964	4.65	-0.0366	9.16	9.16
126	1.06	4.83	-0.058	8.41	8.41
147	1.16	4.99	0.148	7.86	7.86
168	1.25	5.12	0.223	7.43	7.43
189	1.35	5.24	0.300	7.11	7.11
211	1.44	5.35	0.3646	6.85	7.16
232	1.54	5.44	0.4317	6.64	6.85
253	1.63	5.53	0.4885	6.45	6.58
274	1.72	5.62	0.5423	6.3	6.34
295	1.82	5.68	0.5988	6.19	6.13
316	1.94	5.74	0.6626	6.15	5.94
337	2.04	5.82	0.7129	6.07	5.76
358	2.16	5.88	0.770	6.03	5.60
379	2.28	5.93	0.824	6.02	5.46
400	2.41	5.99	0.879	6.03	5.32

Table A.5 Modeling data for 40% fly ash slurry with actual viscosity values and modeled viscosity values

50% fly ash					
Shear Rate (γ) [per sec]	Shear stress (τ) [Pa]	ln (γ)	ln (τ)	Actual apparent viscosity (m Pa-sec)	Calculated viscosity
0.000111	0.0471	-9.10	-3.055	#######	81.20
21.1	2.2	3.049	0.788	106	94.17
42.1	2.76	3.74	1.015	65.5	64.13
63.2	3.16	4.146	1.150	50.1	51.16
84.2	3.53	4.43	1.261	41.9	43.62
105	3.88	4.65	1.355	36.8	38.58
126	4.2	4.83	1.435	33.3	34.86
147	4.5	4.99	1.504	30.5	31.99
168	4.79	5.12	1.566	28.5	29.70
189	5.08	5.24	1.625	26.8	27.82
211	5.36	5.35	1.678	25.5	26.17
232	5.65	5.44	1.731	24.4	24.82
253	5.93	5.53	1.780	23.5	23.65
274	6.2	5.62	1.824	22.7	22.63
295	6.49	5.68	1.870	22	21.72
316	6.76	5.74	1.911	21.4	20.90
337	7.02	5.82	1.948	20.8	20.17
358	7.27	5.88	1.983	20.3	19.50
379	7.54	5.93	2.020	19.9	18.89
400	7.79	5.99	2.053	19.5	18.33

Table A.6 Modeling data for 50% fly ash slurry with actual viscosity values and modeled viscosity values

60% fly ash					
Shear Rate (γ) [per sec]	Shear Stress (τ) [Pa]	ln (γ)	ln (τ)	Actual apparent viscosity (m Pa-sec)	Calculated viscosity
0.0005	0.0658	-7.60	-2.72	#######	4.14 E 5
21.1	15	3.049	2.708	544	746.90
42.1	21.3	3.74	3.058	506	495.76
63.2	25	4.146	3.218	395	389.58
84.2	28.2	4.43	3.339	334	328.60
105	31	4.65	3.433	295	288.26
126	33.5	4.83	3.511	265	258.71
147	35.5	4.99	3.569	241	236.09
168	37.5	5.12	3.624	223	218.11
189	39.1	5.24	3.663	206	203.39
211	40.5	5.35	3.701	192	190.53
232	41.8	5.44	3.732	181	180.10
252	43	5.53	3.761	170	171.48
274	44.2	5.62	3.788	162	163.17
295	45.6	5.68	3.819	155	156.17
316	47	5.74	3.850	149	149.93
337	48.4	5.82	3.879	144	144.32
358	49.4	5.88	3.899	138	139.23
379	50.2	5.93	3.916	133	134.60
400	51.2	5.99	3.935	128	130.36

Table A.7 Modeling data for 60% fly ash slurry with actual viscosity values and modeled viscosity values

65% fly ash slurry					
Shear Rate (γ) [per sec]	Shear Stress (τ) [Pa]	ln (γ)	ln (τ)	Actual apparent viscosity (mPa-sec)	Calculated viscosity
0.000591	0.0658	-7.43	-2.72	#######	3.92 E5
21.1	40.7	3.049	3.706	1930	2219.2
42.1	67.3	3.74	4.209	1600	1577.82
63.2	84.1	4.146	4.432	1330	1291.02
84.2	98.6	4.43	4.591	1170	1120.49
105	110	4.65	4.700	1050	1004.77
126	122	4.83	4.804	966	918.26
147	132	4.99	4.882	899	850.95
168	143	5.12	4.962	847	796.65
189	152	5.24	5.023	805	751.16
211	160	5.35	5.075	758	711.86
232	164	5.44	5.099	709	679.28
253	168	5.53	5.123	665	650.83
274	171	5.62	5.142	625	625.70
295	175	5.68	5.164	593	603.29
316	179	5.74	5.187	567	583.31
337	183	5.82	5.209	543	564.91
358	186	5.88	5.225	520	548.30
379	189	5.93	5.241	498	533.08
400	191	5.99	5.252	477	519.07

Table A.8 Modeling data for 65% fly ash slurry with actual viscosity values and modeled viscosity values

ANNEXURE B

Additive with 60% Fly Ash Slurry

Slurry without additive				
Meas. Pts	Time (sec)	Viscosity (m Pa-sec)	Shear Rate (per sec)	Shear Stress(Pa)
1	6	######	###	0.0658
2	12	544	#	15
3	18	506	21.1	21.3
4	24	395	42.1	25
5	30	334	63.2	28.2
6	36	295	84.2	31
7	42	265	105	33.5
8	48	241	126	35.5
9	54	223	147	37.5
10	60	206	168	39.1
11	66	192	189	40.5
12	72	181	211	41.8
13	78	170	232	43
14	84	162	253	44.2
15	90	155	274	45.6
16	96	149	295	47
17	102	144	316	48.4
18	108	138	337	49.4
19	114	133	358	50.2
20	120	128	379	51.2
			400	
Average		240		38.28

0.5% detergent Ariel				
Meas. Pts	Time (sec)	Viscosity (m Pa-sec)	Shear Rate (per sec)	Shear Stress(Pa)
1	6	######		0.088
2	12	65.9	21.1	1.39
3	18	56.8	42.1	2.39
4	24	53	63.2	3.35
5	30	50.7	84.2	4.27
6	36	50.1	105	5.27
7	42	50.6	126	6.39
8	48	51.4	147	7.58
9	54	51.3	168	8.59
10	60	51.2	189	9.7
11	66	51.6	211	10.9
12	72	51.9	232	12
13	78	52.4	253	13.2
14	84	52.8	274	14.4
15	90	53.4	295	15.7
16	96	53.9	316	17
17	102	54.5	337	18.4
18	108	55.2	358	19.8
19	114	56	379	21.2
20	120	56.6	400	22.6
Average		53.64		11.27

Table B.1 60% slurry without additive and 0.5% detergent Ariel

1% detergent Ariel				
Meas. Pts	Time (sec)	Viscosity (m Pa-sec)	Shear Rate (per sec)	Shear Stress(Pa)
1	6	######	####	0.309
2	12	311	##	6.54
3	8	244	21.1	10.3
4	24	217	42.1	13.7
5	30	203	63.2	17.1
6	36	196	84.2	20.7
7	42	192	105	24.2
8	48	189	126	27.9
9	54	185	147	31.2
10	60	182	168	34.4
11	66	178	189	37.5
12	72	175	211	40.6
13	78	171	232	43.1
14	84	167	253	45.6
15	90	163	274	48.1
16	96	160	295	50.5
17	102	157	316	52.9
18	108	154	337	55.1
19	114	151	358	57.4
20	120	149	379	59.6
			400	
Average		186.52		35.60

1.5% detergent Ariel				
Meas. Pts	Time (sec)	Viscosity (m Pa-sec)	Shear Rate (per sec)	Shear Stress(Pa)
1	6	######	####	0.0407
2	12	128	##	2.69
3	8	98.7	21.1	4.16
4	24	87.1	42.1	5.5
5	30	81.3	63.2	6.84
6	36	78.4	84.2	8.25
7	42	76.3	105	9.64
8	48	75.3	126	11.1
9	54	74.6	147	12.6
10	60	73.9	168	14
11	66	72.5	189	15.3
12	72	71.1	211	16.5
13	78	70.2	232	17.7
14	84	69.6	253	19
15	90	69	274	20.3
16	96	68.9	295	21.8
17	102	68.4	316	23
18	108	68.1	337	24.4
19	114	67.8	358	25.7
20	120	67.7	379	27.1
			400	
Average		77.20		15.03

Table B.2 60% slurry with 1% and 1.5% detergent Ariel

0.5% Glycerol					1% Glycerol				
Meas. Pts	Time (sec)	Viscosity (m Pa-sec)	Shear Rate (per sec)	Shear Stress(Pa)	Meas. Pts	Time (sec)	Viscosity (m Pa-sec)	Shear Rate (per sec)	Shear Stress(Pa)
1	6	######	####	0.00749	1	6	######	####	0.0909
2	12	88	##	1.15	2	12	64	##	13.5
3	8	36.8	21.1	1.4	3	8	43.3	21.1	18.2
4	24	33.2	42.1	1.6	4	24	33.8	42.1	21.3
5	30	25.3	63.2	1.78	5	30	28.5	63.2	24
6	36	21.1	84.2	1.95	6	36	25	84.2	26.3
7	42	18.5	105	2.11	7	42	22.4	105	28.3
8	48	16.7	126	2.27	8	48	20.5	126	30.1
9	54	15.4	147	2.42	9	54	18.9	147	31.8
10	60	14.4	168	2.57	10	60	17.6	168	33.3
11	66	13.6	189	2.71	11	66	16.5	189	34.7
12	72	12.9	211	2.86	12	72	15.5	211	36
13	78	12.3	232	2.99	13	78	14.8	232	37.4
14	84	11.8	253	3.13	14	84	14.1	253	38.5
15	90	11.4	274	3.26	15	90	13.4	274	39.6
16	96	11.1	295	3.4	16	96	12.9	295	40.6
17	102	10.8	316	3.53	17	102	12.4	316	41.6
18	108	10.5	337	3.67	18	108	11.9	337	42.6
19	114	10	358	3.8	19	114	11.5	358	43.5
20	120	9.85	379	3.94	20	120	11.1	379	44.3
			400					400	
Average		20.19		2.60	Average		21.47		32.92

Table B.3 60% slurry with 0.5% and 1% Glycerol

1.5% Glycerol				
Meas. Pts	Time (sec)	Viscosity (m Pa-sec)	Shear Rate (per sec)	Shear Stress(Pa)
1	6	######	###	0.1
2	12	313	#	9.78
3	8	295	21.1	12.4
4	24	225	42.1	14.2
5	30	187	63.2	15.7
6	36	162	84.2	17
7	42	145	105	18.3
8	48	132	126	19.5
9	54	122	147	20.6
10	60	114	168	21.5
11	66	107	189	22.6
12	72	101	211	23.4
13	78	96	232	24.3
14	84	91.6	253	25.1
15	90	87.7	274	25.8
16	96	84.1	295	26.5
17	102	81.4	316	27.4
18	108	78.4	337	28.1
19	114	75.8	358	28.7
20	120	73.4	379	29.4
			400	
Average		135.33		21.59

0.5% PEG				
Meas. Pts	Time (sec)	Viscosity (m Pa-sec)	Shear Rate (per sec)	Shear Stress(Pa)
1	6	######	#####	0.0278
2	12	811	#	17.1
3	8	605	21.1	25.5
4	24	484	42.1	30.6
5	30	413	63.2	34.8
6	36	366	84.2	38.6
7	42	332	105	41.9
8	48	303	126	44.7
9	54	279	147	47.1
10	60	259	168	49.1
11	66	242	189	51
12	72	228	211	52.7
13	78	216	232	54.6
14	84	207	253	56.7
15	90	198	274	58.5
16	96	192	295	60.5
17	102	184	316	62
18	108	177	337	63.2
19	114	170	358	64.5
20	120	165	379	66
			400	
Average		306.89		48.37

Table B.4 60% slurry with 1.5% Glycerol and 0.5% PEG

1% PEG				
Meas. Pts	Time (sec)	Viscosity (m Pa-sec)	Shear Rate (per sec)	Shear Stress(Pa)
1	6	######	####	0.121
2	12	178	##	3.74
3	8	113	21.1	4.78
4	24	87.7	42.1	5.54
5	30	74.1	63.2	6.24
6	36	65.8	84.2	6.93
7	42	60.3	105	7.62
8	48	55.5	126	8.18
9	54	51.9	147	8.74
10	60	48.7	168	9.23
11	66	46.3	189	9.74
12	72	44.3	211	10.3
13	78	42.8	232	10.8
14	84	42	253	11.5
15	90	40.5	274	11.9
16	96	39.2	295	12.4
17	102	37.9	316	12.8
18	108	36.9	337	13.2
19	114	35.8	358	13.6
20	120	34.9	379	14
			400	
Average		59.76		9.53

1.5% PEG				
Meas. Pts	Time (sec)	Viscosity (m Pa-sec)	Shear Rate (per sec)	Shear Stress(Pa)
1	6	######	####	0.0631
2	12	471	##	11.6
3	8	374	21.1	15.7
4	24	298	42.1	18.8
5	30	254	63.2	21.4
6	36	225	84.2	23.7
7	42	204	105	25.8
8	48	189	126	27.8
9	54	176	147	29.6
10	60	166	168	31.4
11	66	157	189	33.1
12	72	151	211	35
13	78	145	232	36.6
14	84	139	253	38.2
15	90	134	274	39.6
16	96	130	295	41
17	102	126	316	42.4
18	108	122	337	43.8
19	114	119	358	45.2
20	120	116	379	46.5
			400	
Average		194.52		31.95

Table B.5 60% slurry with 1% and 1.5% PEG

0.5% SLS				
Meas. Pts	Time (sec)	Viscosity (m Pa-sec)	Shear Rate (per sec)	Shear Stress(Pa)
1	6	######	####	0.388
2	12	16.8	##	0.354
3	8	19.5	21.1	0.822
4	24	23.2	42.1	1.46
5	30	23.8	63.2	2
6	36	25	84.2	2.63
7	42	25.9	105	3.28
8	48	26.3	126	3.87
9	54	26.8	147	4.51
10	60	27.2	168	5.16
11	66	27.7	189	5.84
12	72	28.3	211	6.55
13	78	28.8	232	7.28
14	84	29.4	253	8.03
15	90	29.8	274	8.78
16	96	30.4	295	9.59
17	102	30.4	316	10.2
18	108	30.6	337	11
19	114	30.9	358	11.7
20	120	31	379	12.4
			400	
Average		26.93		6.07

1% SLS				
Meas. Pts	Time (sec)	Viscosity (m Pa-sec)	Shear Rate (per sec)	Shear Stress(Pa)
1	6	######	####	0.318
2	12	15.4	##	0.324
3	8	20.5	21.1	0.862
4	24	22.6	42.1	1.43
5	30	22.8	63.2	1.92
6	36	23.5	84.2	2.47
7	42	24	105	3.04
8	48	24.5	126	3.61
9	54	24.	147	4.15
10	60	25.1	168	4.76
11	66	25.7	189	5.41
12	72	26.1	211	6.05
13	78	26.6	232	6.71
14	84	26.9	253	7.37
15	90	27.3	274	8.05
16	96	27.6	295	8.72
17	102	27.9	316	9.41
18	108	28	337	10
19	114	28.2	358	10.7
20	120	28.2	379	11.3
			400	
Average		24.99		5.59

Table B.6 60% slurry with 0.5% and 1% SLS

1.5% SLS				
Meas. Pts	Time (sec)	Viscosity (m Pa-sec)	Shear Rate (per sec)	Shear Stress(Pa)
1	6	######	######	0.092
2	12	24.9	21.1	0.524
3	8	26	42.1	1.09
4	24	26.1	63.2	1.65
5	30	27.6	84.2	2.32
6	36	28.9	105	3.04
7	42	29.5	126	3.73
8	48	29.5	147	4.34
9	54	29.6	168	4.99
10	60	29.9	189	5.67
11	66	30.5	211	6.42
12	72	30.9	232	7.14
13	78	31.2	253	7.88
14	84	31.5	274	8.63
15	90	31.9	295	9.4
16	96	32.2	316	10.2
17	102	32.4	337	10.9
18	108	32.9	358	11.8
19	114	33.2	379	12.6
20	120	33	400	13.2
Average		28.67		6.60

Table B.7 60% with 1.5% SLS

0.5% Detergent Ariel				Actual apparent viscosity	calculated viscosity
Shear rate (per sec)	Shear stress (Pa)	ln (γ)	ln (τ)		
#####	0.088	######	-2.430	######	#######
21.1	1.39	3.049	0.329	65.9	128.52
42.1	2.39	3.740	0.871	56.8	70.4
63.2	3.35	4.146	1.209	53	49.43
84.2	4.27	4.433	1.452	50.7	38.5
105	5.27	4.654	1.662	50.1	31.76
126	6.39	4.836	1.855	50.6	27.1
147	7.58	4.990	2.026	51.4	23.69
168	8.59	5.124	2.151	51.3	21.09
189	9.7	5.242	2.272	51.2	19.03
211	10.9	5.352	2.389	51.6	17.29
232	12	5.447	2.485	51.9	15.96
253	13.2	5.533	2.580	52.4	14.8
274	14.4	5.613	2.667	52.8	13.8
295	15.7	5.687	2.754	53.4	12.94
316	17	5.756	2.833	53.9	12.19
337	18.4	5.820	2.912	54.5	11.53
358	19.8	5.881	2.986	55.2	10.91
379	21.2	5.938	3.054	56	10.41
400	22.6	5.991	3.118	56.6	9.93

Table B.8 Modelling data of 60% fly ash concentration with 0.5% detergent Ariel

1% Detergent Ariel				Actual apparent viscosity	calculated viscosity
Shear rate (per sec)	Shear stress (Pa)	ln (γ)	ln (τ)		
	0.309		-1.174		
21.1	6.54	3.049	1.878	311	310.3
42.1	10.3	3.740	2.332	244	261.63
63.2	13.7	4.146	2.617	217	236.65
84.2	17.1	4.433	2.839	203	220.46
105	20.7	4.654	3.030	196	208.76
126	24.2	4.836	3.186	192	199.56
147	27.9	4.990	3.329	189	192.11
168	31.2	5.124	3.440	185	185.88
189	34.4	5.242	3.538	182	180.55
211	37.5	5.352	3.624	178	175.7
232	40.6	5.447	3.704	175	171.63
253	43.1	5.533	3.764	171	168
274	45.6	5.613	3.820	167	164.72
295	48.1	5.687	3.873	163	161.74
316	50.5	5.756	3.922	160	159.02
337	52.9	5.820	3.968	157	156.51
358	55.1	5.881	4.009	154	154.19
379	57.4	5.938	4.050	151	152.04
400	59.6	5.991	4.088	149	150.02

Table B.9 Modelling data of 60% fly ash concentration with 1% detergent Ariel

1.5% Detergent Ariel				Actual apparent viscosity	calculated viscosity
Shear rate (per sec)	Shear stress (Pa)	ln (γ)	ln (τ)		
######	0.0407	######	-3.202	######	#######
21.1	2.69	3.049	0.990	128	125.38
42.1	4.16	3.740	1.426	98.7	107.33
63.2	5.5	4.146	1.705	87.1	97.95
84.2	6.84	4.433	1.923	81.3	91.83
105	8.25	4.654	2.110	78.4	87.38
126	9.64	4.836	2.266	76.3	83.87
147	11.1	4.990	2.407	75.3	81.01
168	12.6	5.124	2.534	74.6	78.81
189	14	5.242	2.639	73.9	76.55
211	15.3	5.352	2.728	72.5	74.68
232	16.5	5.447	2.803	71.1	73.1
253	17.7	5.533	2.874	70.2	71.69
274	19	5.613	2.944	69.6	70.42
295	20.3	5.687	3.011	69	69.26
316	21.8	5.756	3.082	68.9	68.19
337	23	5.820	3.135	68.4	67.21
358	24.4	5.881	3.195	68.1	66.3
379	25.7	5.938	3.246	67.8	65.46
400	27.1	5.991	3.300	67.7	64.67

Table B.10 Modelling data of 60% fly ash concentration with 1.5% detergent Ariel

0.5% Glycerol				Actual apparent viscosity	calculated viscosity
Shear rate (per sec)	Shear stress (Pa)	ln (γ)	ln (τ)		
#####	0.00749	#####	-4.894	#####	#####
21.1	1.15	3.049	0.140	88	53.67
42.1	1.4	3.740	0.336	36.8	35.62
63.2	1.6	4.146	0.470	33.2	27.98
84.2	1.78	4.433	0.577	25.3	23.6
105	1.95	4.654	0.668	21.1	20.7
126	2.11	4.836	0.747	18.5	18.58
147	2.27	4.990	0.820	16.7	16.95
168	2.42	5.124	0.884	15.4	15.66
189	2.57	5.242	0.944	14.4	14.66
211	2.71	5.352	0.997	13.6	13.68
232	2.86	5.447	1.051	12.9	12.93
253	2.99	5.533	1.095	12.3	12.28
274	3.13	5.613	1.141	11.8	11.71
295	3.26	5.687	1.182	11.4	11.21
316	3.4	5.756	1.224	11.1	10.76
337	3.53	5.820	1.261	10.8	10.36
358	3.67	5.881	1.300	10.5	9.99
379	3.8	5.938	1.335	10	9.66
400	3.94	5.991	1.371	9.85	9.36

Table B.11 Modelling data of 60% fly ash concentration with 0.5% Glycerol

1% Glycerol				Actual apparent viscosity	calculated viscosity
Shear rate (per sec)	Shear stress (Pa)	ln (γ)	ln (τ)		
#####	0.0909	#####	-2.398	#####	#####
21.1	13.5	3.049	2.603	64	64.11
42.1	18.2	3.740	2.901	43.3	42.52
63.2	21.3	4.146	3.059	33.8	33.4
84.2	24	4.433	3.178	28.5	28.16
105	26.3	4.654	3.270	25	24.7
126	28.3	4.836	3.343	22.4	22.16
147	30.1	4.990	3.405	20.5	20.22
168	31.8	5.124	3.459	18.9	18.68
189	33.3	5.242	3.506	17.6	17.42
211	34.7	5.352	3.547	16.5	16.31
232	36	5.447	3.584	15.5	15.42
253	37.4	5.533	3.622	14.8	14.64
274	38.5	5.613	3.651	14.1	13.96
295	39.6	5.687	3.679	13.4	13.37
316	40.6	5.756	3.704	12.9	12.83
337	41.6	5.820	3.728	12.4	12.35
358	42.6	5.881	3.752	11.9	11.91
379	43.5	5.938	3.773	11.5	11.52
400	44.3	5.991	3.791	11.1	11.15

Table B.12 Modelling data of 60% fly ash concentration with 1% Glycerol

1.5 % Glycerol				Actual apparent viscosity	calculated viscosity
Shear rate (per sec)	Shear stress (Pa)	ln (γ)	ln (τ)		
#####	0.1	#####	-2.303	#####	#####
21.1	9.78	3.049	2.280	313	624.1
42.1	12.4	3.740	2.518	295	404.3
63.2	14.2	4.146	2.653	225	313.19
84.2	15.7	4.433	2.754	187	261.52
105	17	4.654	2.833	162	227.52
126	18.3	4.836	2.907	145	202.99
147	19.5	4.990	2.970	132	184.25
168	20.6	5.124	3.025	122	169.41
189	21.5	5.242	3.068	114	157.33
211	22.6	5.352	3.118	107	146.81
232	23.4	5.447	3.153	101	138.31
253	24.3	5.533	3.190	96	130.98
274	25.1	5.613	3.223	91.6	124.57
295	25.8	5.687	3.250	87.7	118.92
316	26.5	5.756	3.277	84.1	113.89
337	27.4	5.820	3.311	81.4	109.38
358	28.1	5.881	3.336	78.4	105.3
379	28.7	5.938	3.357	75.8	101.6
400	29.4	5.991	3.381	73.4	98.21

Table B.13 Modelling data of 60% fly ash concentration with 1.5% Glycerol

0.5% PEG				Actual apparent viscosity	calculated viscosity
Shear rate (per sec)	Shear stress (Pa)	ln (γ)	ln (τ)		
#####	0.0278	#####	-3.583	#####	#####
21.1	17.1	3.049	2.839	811	814.17
42.1	25.5	3.740	3.239	605	561.92
63.2	30.6	4.146	3.421	484	451.82
84.2	34.8	4.433	3.550	413	387.33
105	38.6	4.654	3.653	366	344.04
126	41.9	4.836	3.735	332	311.96
147	44.7	4.990	3.800	303	287.19
168	47.1	5.124	3.852	279	267.32
189	49.1	5.242	3.894	259	250.94
211	51	5.352	3.932	242	236.54
232	52.7	5.447	3.965	228	224.8
253	54.6	5.533	4.000	216	214.58
274	56.7	5.613	4.038	207	205.59
295	58.5	5.687	4.069	198	197.6
316	60.5	5.756	4.103	192	190.44
337	62	5.820	4.127	184	183.97
358	63.2	5.881	4.146	177	178.1
379	64.5	5.938	4.167	170	172.73
400	66	5.991	4.190	165	167.8

Table B.14 Modelling data of 60% fly ash concentration with 0.5% PEG

1% PEG				Actual apparent viscosity	calculated viscosity
Shear rate (per sec)	Shear stress (Pa)	ln (γ)	ln (τ)		
#####	0.121	#####	-2.112	#####	#####
21.1	3.74	3.049	1.319	178	175.49
42.1	4.78	3.740	1.564	113	119.15
63.2	5.54	4.146	1.712	87.7	94.9
84.2	6.24	4.433	1.831	74.1	80.81
105	6.93	4.654	1.936	65.8	71.41
126	7.62	4.836	2.031	60.3	64.48
147	8.18	4.990	2.102	55.5	59.15
168	8.74	5.124	2.168	51.9	54.88
189	9.23	5.242	2.222	48.7	51.38
211	9.74	5.352	2.276	46.3	48.31
232	10.3	5.447	2.332	44.3	45.81
253	10.8	5.533	2.380	42.8	43.54
274	11.5	5.613	2.442	42	41.73
295	11.9	5.687	2.477	40.5	40.04
316	12.4	5.756	2.518	39.2	38.53
337	12.8	5.820	2.549	37.9	37.16
358	13.2	5.881	2.580	36.9	35.92
379	13.6	5.938	2.610	35.8	34.8
400	14	5.991	2.639	34.9	33.76

Table B.15 Modelling data of 60% fly ash concentration with 1% PEG

1.5% PEG				Actual apparent viscosity	calculated viscosity
Shear rate (per sec)	Shear stress (Pa)	ln (γ)	ln (τ)		
#####	0.0631	#####	-2.763	#####	#####
21.1	11.6	3.049	2.451	471	546.92
42.1	15.7	3.740	2.754	374	378.59
63.2	18.8	4.146	2.934	298	304.94
84.2	21.4	4.433	3.063	254	261.74
105	23.7	4.654	3.165	225	232.71
126	25.8	4.836	3.250	204	211.18
147	27.8	4.990	3.325	189	194.54
168	29.6	5.124	3.388	176	181.18
189	31.4	5.242	3.447	166	170.17
211	33.1	5.352	3.500	157	160.48
232	35	5.447	3.555	151	152.57
253	36.6	5.533	3.600	145	145.69
274	38.2	5.613	3.643	139	139.63
295	39.6	5.687	3.679	134	134.25
316	41	5.756	3.714	130	129.42
337	42.4	5.820	3.747	126	125.06
358	43.8	5.881	3.780	122	121.1
379	45.2	5.938	3.811	119	117.48
400	46.5	5.991	3.839	116	114.15

Table B.16 Modeling data of 60% fly ash concentration with 1.5% PEG

0.5% SLS				Actual apparent viscosity	calculated viscosity
Shear rate (per sec)	Shear stress (Pa)	ln (γ)	ln (τ)		
#####	0.388	######	-0.947	######	######
21.1	0.354	3.049	-1.038	16.8	16.7
42.1	0.822	3.740	-0.196	19.5	19.3
63.2	1.46	4.146	0.378	23.2	21.1
84.2	2	4.433	0.693	23.8	22.42
105	2.63	4.654	0.967	25	23.49
126	3.28	4.836	1.188	25.9	24.41
147	3.87	4.990	1.353	26.3	25.52
168	4.51	5.124	1.506	26.8	25.94
189	5.16	5.242	1.641	27.2	26.59
211	5.84	5.352	1.765	27.7	27.22
232	6.55	5.447	1.879	28.3	27.77
253	7.28	5.533	1.985	28.8	28.28
274	8.03	5.613	2.083	29.4	28.76
295	8.78	5.687	2.172	29.8	29.21
316	9.59	5.756	2.261	30.4	29.64
337	10.2	5.820	2.322	30.4	30.04
358	11	5.881	2.398	30.6	30.43
379	11.7	5.938	2.460	30.9	30.8
400	12.4	5.991	2.518	31	31.15

Table B.17 Modelling data of 60% fly ash concentration with 0.5% SLS

1% SLS				Actual apparent viscosity	calculated viscosity
Shear rate (per sec)	Shear stress (Pa)	ln (γ)	ln (τ)		
####	0.318	#####	-1.146	#####	######
21.1	0.324	3.049	-1.127	15.4	15.4
42.1	0.862	3.740	-0.149	20.5	17.83
63.2	1.43	4.146	0.358	22.6	19.42
84.2	1.92	4.433	0.652	22.8	20.64
105	2.47	4.654	0.904	23.5	21.62
126	3.04	4.836	1.112	24	22.47
147	3.61	4.990	1.284	24.5	23.22
168	4.15	5.124	1.423	24	23.88
189	4.76	5.242	1.560	25.1	24.48
211	5.41	5.352	1.688	25.7	25.06
232	6.05	5.447	1.800	26.1	25.57
253	6.71	5.533	1.904	26.6	26.04
274	7.37	5.613	1.997	26.9	26.48
295	8.05	5.687	2.086	27.3	26.9
316	8.72	5.756	2.166	27.6	27.29
337	9.41	5.820	2.242	27.9	27.67
358	10	5.881	2.303	28	28.02
379	10.7	5.938	2.370	28.2	28.36
400	11.3	5.991	2.425	28.2	28.69

Table B.18 Modelling data of 60% fly ash concentration with 1% SLS

1.5% SLS				Actual apparent viscosity	calculated viscosity
Shear rate (per sec)	Shear stress (Pa)	ln (γ)	ln (τ)		
#####	0.092	#####	-2.386	#######	######
21.1	0.524	3.049	-0.646	24.9	24.76
42.1	1.09	3.740	0.086	26	26.64
63.2	1.65	4.146	0.501	26.1	27.46
84.2	2.32	4.433	0.842	27.6	28.22
105	3.04	4.654	1.112	28.9	28.81
126	3.73	4.836	1.316	29.5	29.31
147	4.34	4.990	1.468	29.5	29.74
168	4.99	5.124	1.607	29.6	30.12
189	5.67	5.242	1.735	29.9	30.45
211	6.42	5.352	1.859	30.5	30.77
232	7.14	5.447	1.966	30.9	31.05
253	7.88	5.533	2.064	31.2	31.3
274	8.63	5.613	2.155	31.5	31.54
295	9.4	5.687	2.241	31.9	31.76
316	10.2	5.756	2.322	32.2	31.97
337	10.9	5.820	2.389	32.4	32.16
358	11.8	5.881	2.468	32.9	32.35
379	12.6	5.938	2.534	33.2	32.52
400	13.2	5.991	2.580	33	32.69

Table B.19 Modelling data of 60% fly ash concentration with 1.5% SLS

ANNEXURE C

PARTICLE SIZE DISTRIBUTION

Mechanical Sieving of Fly ash

Weight of pan	139.23 grams
Weight of fly ash	200 grams
Time of sieving	10 minutes

Sieve Size (British Standard)	Sieve size	Particle size (µm)	Fly ash Without Pan (grams)	Weight %	Cumulative wt. % finer
8	2000 µm	2000	0.12	0.217144	99.79
10	1700µm	1700 to 2000	0.42	3.22614	96.56
16	1000 µm	1000 to 1700	6.24	2.6936201	93.87
22	710 µm	710 to 1000	5.21	4.1464171	89.73
30	500 µm	500 to 710	8.02	1.994623	88.54
44	355 µm	355 to 500	2.32	1.2149726	87.33
60	250 µm	250 to 355	2.35	4.2136284	83.12
100	150 µm	150 to 250	8.15	7.8688864	75.26
150	106 µm	106 to 150	15.22	23.58629	52.21
200	75 µm	75 to 106	44.6	48.169786	4.05
300	53 µm	53 to 75	93.17	3.9292731	0.13
pan	<53 µm	0 to 53	7.6	0	0

Table C.1 Data obtained during calculation of particle size distribution (PSD) of Fly ash